The discovery of the heaviest elements

S. Hofmann and G. Münzenberg

Gesellschaft für Schwerionenforschung mbH (GSI), D-64291 Darmstadt, Germany

The nuclear shell model predicts that the next doubly magic shell closure beyond ^{208}Pb is at a proton number between $Z=114$ and 126 and at a neutron number $N=184$. The outstanding aim of experimental investigations is the exploration of this region of spherical superheavy elements (SHE's). This article describes the experimental methods that led to the identification of elements 107 to 112 at GSI, Darmstadt. Excitation functions were measured for the one-neutron evaporation channel of cold-fusion reactions using lead and bismuth targets. The maximum cross section was measured at beam energies well below a fusion barrier estimated in one dimension. These studies indicate that the transfer of nucleons is an important process for the initiation of fusion. The recent efforts at JINR, Dubna, to investigate the hot-fusion reaction for the production of SHE's using actinide targets are also presented. First results were obtained on the synthesis of neutron-rich isotopes of elements 112 and 114. However, the most surprising result was achieved in 1999 at LBNL, Berkeley. In a study of the reaction ^{86}Kr+^{208}Pb$\rightarrow^{294}$118*, three decay chains were measured and assigned to the superheavy nucleus ^{293}118. The decay data reveal that, for the heaviest elements, the dominant decay mode is alpha emission, not fission. The results are discussed in the framework of theoretical models. This article also presents plans for the further development of the experimental setup and the application of new techniques. At a higher sensitivity, the exploration of the region of spherical SHE's now seems to be feasible, more than 30 years after its prediction.

CONTENTS

ABBREVIATIONS FOR FACILITIES AND EXPERIMENTS

ATLAS	Argonne Tandem Linac Accelerator System, superconducting accelerator for projectiles heavier than the electron at Argonne National Laboratory, Argonne, Illinois, USA
ANL	Argonne National Laboratory
BGS	Berkeley Gas-filled Separator at LBNL in Berkeley, California, USA
CAPRICE	Compacte A Plusieurs Résonances Ionisantes Cyclotron, special type of Electron Cyclotron Resonance (ECR) ion source
EXCYT	Exotics with Cyclotron and Tandem is the development of a facility for producing and accelerating exotic beams up to 8 MeV/amu. The laboratory is located in Catania, Italy
FLNR	Flerov Laboratory of Nuclear Reactions at JINR in Dubna, Russia
FMA	Fragment Mass Analyzer
GANIL	Grand Accelerateur National d'Ions Lourds, Accelerator Laboratory in Caen, France
GNS	The Dubna gas-filled separator. GNS stands for ''Gaso Napolnennyj Separator,'' the Russian expression for gas-filled separator
GSI	Gesellschaft für Schwer-Ionen-Forschung, Accelerator laboratory in Darmstadt, Germany
HILAC	Heavy Ion Linear Accelerator at LBNL in Berkeley, California
JHF	Japanese Hadron Facility
JINR	Joint Institute for Nuclear Research in Dubna 130 km north from Moscow
JYFL	Jyväskylän Yliopiston Fysiikan Laitos, the Finnish words for University of Jyväskylä, Department of Physics, an accelerator Laboratory in Jyväskylä, Finland

LASSY	Large Angle Separator SYstem, planned, but rejected gas-filled separator at LBNL in Berkeley, California, USA
LBNL	Lawrence Berkeley National Laboratory in Berkeley, California, USA
LLNL	Lawrence Livermore National Laboratory in Livermore, California, USA
MAFF	Munich Accelerator for Fission Fragments, Munich radioactive nuclear beam project for the acceleration of fission fragments produced in a reactor
OLGA	On-Line Gas chromatography Apparatus
RIA	Rare Isotope Accelerator, accelerator project in the USA
RIKEN	Institute of Physical and Chemical Research in Saitama near Tokyo, Japan
RITU	A Finnish woman's name and stands for Recoil Ion Transport Unit
SHIP	Separator for Heavy Ion reaction Products, velocity filter for fusion reaction products at GSI, Darmstadt, Germany
SPIRAL	Système de Production d'Ions Radioactifs et d'Accélération en Ligne, an accelerator complex for the production and acceleration of radioactive ions under construction at GANIL in Caen, France
UNILAC	UNIversal Linear ACcelerator, an accelerator for heavy ions at GSI in Darmstadt, Germany
VASSILISSA	Separator for fusion-reaction products named after a fairy in a Russian fairy tale
VEGA	Versatile and Efficient GAmma detectors, a gamma-detector array under construction at GSI in Darmstadt, Germany

I. INTRODUCTION

Searching for new elements is an attempt to answer questions of partly fundamental character: How many elements may exist? How long is their lifetime? Which properties determine their stability? How can they be synthesized? What are their chemical properties? How are the electrons arranged in the strong electric field of the nucleus?

When searching for new elements beyond uranium by the process of neutron capture and subsequent β^- decay, Hahn and Strassmann (1939) discovered the possibility that a heavy nucleus might ''divide itself into two nuclei.'' This was the correct interpretation given by Meitner and Frisch (1939), and the term ''fission'' was coined for this process. By applying the existing charged liquid-drop model of the nucleus (Gamov, 1930), nuclear fission was explained quite naturally, and it was shown that fission will most likely limit the number of chemical elements. The maximum number of elements could be expected to be 100–125. These numbers result from the balance of two fundamental nuclear parameters, the strength of the attractive nuclear surface tension and the repulsive electric force.

The properties of nuclei are not smooth, uniform functions of the proton and neutron numbers, but show nonuniformities, as evidenced by the measured atomic masses. At the ''magic'' proton or neutron numbers 2, 8, 20, 28, 50, and 82, the nuclei have an increased binding energy relative to the average trend. For neutrons, $N=126$ is also identified as a magic number. However, the highest stability is observed in the case of the doubly magic nuclei. Amongst other special properties, the doubly magic nuclei are spherical and resist deformation.

The magic numbers were successfully explained by the nuclear shell model (Göppert-Mayer, 1948; Haxel *et al.*, 1949; Göppert-Mayer and Jensen, 1955). The correct level splitting was obtained with a spin-orbit term in the nuclear potential. The numbers 126 for the protons and 184 for the neutrons were predicted to be the next shell closures.

The prediction of magic numbers was less problematic than the calculation of the stability of those doubly closed shell nuclei against fission. At the largest deformation, involved in the calculation of the fission barrier, the surface energy could not be treated correctly using the single-particle shell model. It was Strutinsky (1967) who considered the shell effect as a small deviation from a uniform single-particle energy-level distribution. This deviation was then used as a correction to the liquid-drop model energy.

A series of papers have based calculations of the location and properties of superheavy elements (SHE's) on the Strutinsky shell-correction method (Myers and Świątecki, 1966; Meldner, 1967; Nilsson *et al.*, 1968; Mosel and Greiner, 1969; Fiset and Nix, 1972; Randrup *et al.*, 1976). Most of the calculations were in agreement that $N=184$ would be the next magic neutron number, but for the protons, both $Z=114$ and 126 were suggested as magic numbers. The element with $Z=114$ has found support in recent models based on the Strutinsky approach (Möller and Nix, 1994; Sobiczewski, 1994; Smolanczuk *et al.*, 1995), whereas Hartree-Fock calculations predict the highest stability at a proton number $Z=120$ (Rutz *et al.*, 1997) or $Z=126$ (Ćwiok *et al.*, 1996). The reason for this uncertainty lies in the difficulty involved in localizing the energies of the single-particle levels between $Z=114$ and 126, a problem that is caused mainly by the uncertain strength of the spin-orbit coupling. The different numbers predicted for the closed proton shell may also suggest that the structure of the shell-correction energy landscape of nuclei in the region of SHE's may differ from those in the vicinity of ^{208}Pb. This result was already evidenced in early calculations (see, for example, Nilsson *et al.*, 1969). Instead of a sharp minimum at the magic proton and neutron number, a wider range of less pronounced negative shell-correction energies was calculated expanding from $Z=114$ to 126 and $N=184$ to 196.

As a consequence, the predicted half-lives based on the various calculations differed by many orders of mag-

nitude. Some of the half-lives approached the age of the universe, and attempts have been made to discover naturally occurring superheavy elements. Terrestrial as well as extraterrestrial materials have been investigated. The latter came to the laboratories in the form of meteorites or were collected during missions to the moon. Although discoveries were announced from time to time, none could be substantiated after closer inspection.

The most successful methods for the laboratory synthesis of heavy elements have been fusion-evaporation reactions using heavy-element targets, recoil-separation techniques, and the identification of the nuclei by generic ties to known daughter decays after implantation into position-sensitive detectors. Experiments at low cross sections necessitate projectile beams of high density and stability. Although the intensity limits have not at present been reached, considerable improvements have been made in recent years.

In the following section we give a more detailed description of the experimental setup that has been used at the Gesellschaft für Schwerionenforschung (GSI) in Darmstadt for the identification of elements 107 to 112. In addition, we give an overview of facilities in various laboratories where experiments for the investigation of heavy elements are being performed. Additional sections are devoted to properties of neutron-rich and neutron-deficient isotopes and to the recent in-beam gamma ray experiments. The recent results obtained at the Joint Insitute for Nuclear Research (JINR), Dubna, from studies of hot-fusion reaction producing nuclei up to element 114 are described, as are the sensational results reported by experimentalists at Lawrence Berkeley National Laboratory (LBNL), Berkeley, on the synthesis of element 118, using cold fusion. The decay data are compared with predictions of theoretical models and, in Sec. V, phenomena influencing the cross section for the synthesis of SHE's are discussed. Finally, a summary and outlook are given and, in the Appendix, the naming of the elements is discussed.

II. TECHNIQUES FOR THE DISCOVERY OF NEW ELEMENTS

The transuranium elements were produced artificially. Up to fermium, neutron capture in high-flux reactors and successive β^- decay makes it possible to climb up the periodic table element by element. At fermium, however, this process ends due to the short α and fission half-lives of the heavier elements. While from neptunium to californium some isotopes can be produced in amounts measured in kilograms or at least grams, the two heaviest species, ^{254}Es and ^{257}Fm, are available only in quantities of micrograms and picograms, respectively.

The region beyond fermium is best accessible using heavy-ion reactions, the bombardment of heavy-element targets with heavy ions from an accelerator. The cross section is less than in the case of neutron capture, and values are considerably below the geometrical size of the nuclei. Moreover, only thin targets of the order of 1 mg/cm^2 can be used. This limitation arises from the energy loss of the ion beam in the target, which results (using thicker targets) in an energy distribution that is too wide for either the production of fusion products or their in-flight separation.

On the other hand, the use of thin targets in combination with well-defined beam energies from accelerators results in unique information about the reaction mechanism. The data are obtained by measuring excitation functions, the cross section as a function of the beam energy.

Various combinations of projectiles and targets are in principle possible for the synthesis of heavy elements: actinide targets irradiated by light projectiles of elements from neon to calcium, targets of lead and bismuth irradiated by projectiles from calcium to krypton, and symmetric combinations, like tin plus tin, up to samarium plus samarium.

Historically, the first accelerators used for the production of heavy elements were the cyclotrons in Berkeley, California, and later in Dubna, Russia. They were only able to accelerate light ions up to about neon with sufficient intensity and up to an energy high enough for fusion reactions. Larger and more powerful cyclotrons were built in Dubna for the investigation of reactions using projectiles near calcium. These were the U300 and U400, 300- and 400-cm-diameter cyclotrons. In Berkeley a linear accelerator, HILAC (Heavy-Ion Linear Accelerator), later upgraded to the SuperHILAC, was built. The shutdown of this accelerator in 1992 led to a revival of heavy-element experiments at the 88-in. cyclotron. Aiming at the acceleration of ions as heavy as uranium, the UNILAC (Universal Linear Accelerator) was constructed in Darmstadt, Germany.

In order to compensate for the decreasing cross sections of the synthesis of heavy elements, increasing beam currents are needed from the accelerators. This demands a continuous development of ion sources in order to deliver high currents at high ionic charge states. In the following, we shall describe the efforts that have been made in recent years at the UNILAC to achieve this aim. The developments in the laboratories in Berkeley, and Dubna and also in Finland, France, Italy, and Japan are similar and are usually made in close collaboration, with an exchange of know-how. The development and construction of separators and detector systems proceed in a similar fashion. As a prime example of such instruments, we shall describe in the following the velocity filter SHIP (Separator for Heavy-Ion Reaction Products) and its detector system, which were developed at the UNILAC. Both the principle of separation and the detection techniques used in the other laboratories are comparable.

A. Ion source and accelerator

At the UNILAC, the facilities for experiments at low projectile energies were upgraded a few years ago. A new high-charge injector was built, including a 14-GHz-ECR (electron cyclotron resonance) CAPRICE-type

ion source (Geller *et al.*, 1992). The ion source is followed by a radio-frequency quadrupole and an interdigital *H*-structure accelerator that provide a beam energy of 1.4 MeV/u (MeV per mass unit u) for direct injection into the Alvarez section of the UNILAC (Angert *et al.*, 1989). The advantages, compared with the previously used Penning ion source are

(1) Low consumption of material ($\approx$0.2–4 mg/h).

(2) Intense and stable projectile currents.

(3) A high-quality beam of low emittance, halo free and of well-defined energy.

The high beam quality is a result of the high ionic charge state attained (10^+ in the case of ^{70}Zn; Bossler *et al.*, 1997). This charge state is maintained throughout the acceleration process—an increase by stripping of electrons is unnecessary. The reduction of projectile background behind the SHIP is partially due to the increased beam quality.

The beam energy is variable and defined by a set of single resonators. The relative accuracy of the beam energy is ± 0.003 MeV/u. The absolute energies are accurate to ± 0.01 MeV/u. This high accuracy is sufficient for the measurement of narrow excitation functions, as observed for the $1n$ and $2n$ emission channels in reactions for the production of heavy elements.

The beam intensities are rather high and are partly beyond the limits set by the presently used lead or bismuth targets, which melt at low temperature. For example, the following values could be obtained at the target: 3.0 pμA for $^{40}Ar^{8+}$, 1.2 pμA for $^{58}Fe^{8+}$, and 0.4 pμA for $^{82}Se^{12+}$ (1 pμA$=6.24\times10^{12}$ particles/s). In the case of rare isotopic abundance, the source material was enriched to reach a concentration higher than 90%.

B. Recoil-separation techniques

In contrast to the recoil-stopping methods, as used in mass separators, where ion sources or He-jet systems are utilized, recoil-separation techniques use the ionic charge and momentum of the recoiling fusion product obtained in the reaction process. Spatial separation from the projectiles and other reaction products is achieved by combined electric and magnetic fields. The separation times are determined by the recoil velocities and the lengths of the separators. They are typically in the range of 1–2 microseconds. Two types of recoil separators have been developed.

(1) The gas-filled separators use the different magnetic rigidities of the recoils and projectiles traveling through a low-pressure (about 1 mbar) gas-filled volume in a magnetic dipole field (Armbruster *et al.*, 1971). In general, helium is used in order to obtain a maximum difference in the rigidities of slow reaction products and fast projectiles. Instruments that have been used in experiments to separate heavy elements were built at GSI, Darmstadt (Berthes, 1987; Ninov *et al.*, 1995), RIKEN, Saitama (Miyatake *et al.*, 1987), LBNL, Berkeley (Ghiorso *et al.*, 1988, Ninov *et al.*, 1998), ANL, Argonne (Paul *et al.*, 1989), JINR, Dubna (Lazarev *et al.*, 1993), and JYFL, Jyväskylä (Leino *et al.*, 1994).

(2) Wien-filter or energy separators use the specific kinematic properties of the fusion products. The latter are created with velocities and energies different from the projectiles and other reaction products. Their ionic charge state is determined when they escape from a thin solid-state target into vacuum. Ionic-charge achromaticity is essential for high transmission. It is achieved by additional magnetic fields or symmetric arrangements of electric fields. Examples of such separators used in experiments for the investigation of heavy elements are the velocity filter SHIP at Darmstadt (Münzenberg *et al.*, 1979) and the recoil-energy separator VASSILISSA at Dubna (Yeremin *et al.*, 1989). The Fragment Mass Analyzer (FMA) at Argonne (Davids, 1992) provides a mass separation of the fusion products. A detailed description of various currently working separators was given by Münzenberg (1997).

To proceed to the region of new elements beyond 109, SHIP was modified and a new improved detection system was built (see Fig. 1). The aims of the SHIP modifications were as follows:

(1) To increase the solid angle and thus increase the transmission of fusion-reaction products. A 50% gain in transmission was achieved by placing the target as close as possible to the first quadrupole triplet.

(2) To reduce the background in order to accept higher beam currents and to simultaneously increase the significance of detected correlated events. The main contributions to the background (energetic ions, which are implanted into the detector in addition to the fusion-reaction products) are high- and low-energy projectiles and transfer products. When the projectiles pass through the target, their ionic charge states are increased by stripping, which causes them to be deflected to the beam stop by the electromagnetic fields of the separator. A fraction of the low-charge projectiles is derived either from the Gaussian-like charge-state distribution or from incomplete or no-charge-state equilibration, e.g., from inhomogeneous targets or targets with pinholes. If the charge state is too low, the rigidity of the ions is high, and these projectiles may reach the detector. A significant reduction of this contribution to the background was obtained by placing an additional 7.5° deflection magnet behind SHIP. The high-energy projectiles were reduced to $\approx$1 count/min over the entire focal plane at a beam current of 1 pμA. Their distribution decreased from the right towards the center of the detector; see Fig. 1.

The low-energy projectile background is due to projectiles that have the same velocity as the reaction products and can therefore pass through the velocity filter. It turned out that the main sources of this contribution to the background were poor beam quality, poor target quality, and interaction of the beam halo with the target frame. At the UNILAC, the beam quality was considerably improved when a single charge state from the electron cyclotron resonance source was accelerated without stripping to higher charge states at medium energy. To avoid scattering at the target frame, the size of the targets was enlarged and the target quality was improved

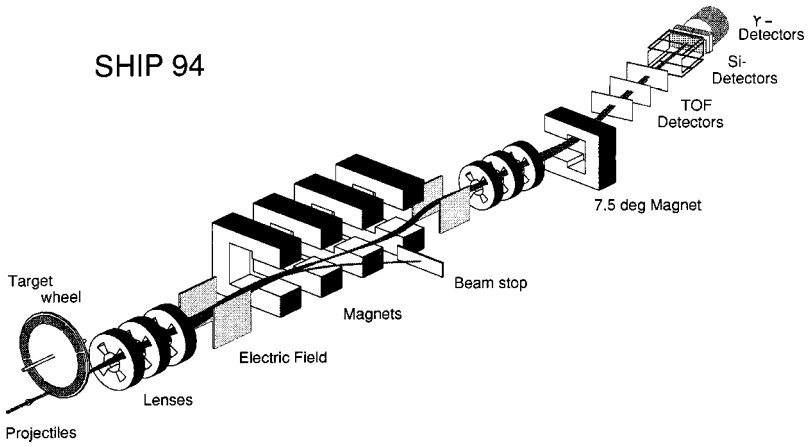

FIG. 1. The modified velocity filter SHIP (Separator for Heavy-Ion Reaction Products, Münzenberg *et al.*, 1979) and the new detection system. The drawing is approximately to scale, but the target wheel and the detectors are enlarged by a factor of 2. The length of SHIP from the target to the detector is 11 m. The target wheel has a radius of 155 mm. It rotates synchronously with beam macrostructure at 1125 rpm (Folger *et al.*, 1995). The detector system consists of three large-area secondary-electron time-of-flight detectors (Śaro *et al.*, 1996) and a position-sensitive silicon detector array (Hofmann *et al.*, 1995a). The flight time of the reaction products through SHIP is 2 μs. The filter, comprised of two electric and four magnetic dipole fields plus two quadrupole triplets, was extended by a fifth deflection magnet, allowing for the positioning of the detectors away from the straight beam line and for further reduction of the background.

(Folger *et al.*, 1995). The low-energy projectiles passing through the SHIP have a lower magnetic rigidity than the reaction products and are deflected to the left side of the detector array. The counting rate is $\approx$30 ions/s at a beam current of 1 p μA ^{58}Fe. This increases for heavier projectiles and reaches values up to $\approx$200 ions/s for ^{86}Kr.

The background due to transfer products is focused towards the center of the detector. The counting rate at a current of 1 p μA is $\approx$1 ion/min.

(3) To stabilize all components of the experimental setup (UNILAC plus SHIP plus detection system) in order to obtain a higher overall duty factor, which means a minimum of losses due to technical failures. In general, a duty factor of 85% is now reached, compared with 65% in previous experiments. The remaining 15% of the time is still needed for changing of the material in the ion source and changing of the target wheel, which should take place approximately every five days.

The sum of these improvements resulted in a sensitivity for detection of one heavy-element decay chain in five days on average, at a beam current of 0.5 p μA and a cross section of 1 pb.

C. Detectors

Recoil separators are designed to filter out nuclei produced in fusion reactions with a high rate of transmission. Since higher yields also produce increased background levels, the transmitted particles have to be identified by detector systems. The detector type to be selected depends on the particle rate, energy, decay mode, and half-life. Experimental as well as theoretical data on the stability of heavy nuclei show that they decay by α emission or electron capture or fission, with half-lives ranging from microseconds to days. Therefore silicon semiconductor detectors are well suited for the identification of nuclei and for the measurement of their decay properties.

If the total rate of ions striking the focal plane of the separator is low, then the particles can be implanted directly into the silicon detectors. Using position-sensitive detectors, one can measure the local distribution of the implanted particles. In this case, the detectors act as diagnostic elements to optimize and control the ion optical properties of the separator.

Given that the implanted nuclei are radioactive, the positions measured for the implantation and all subsequent decay processes are the same. This is the case because the recoil effects are small compared with the range of implanted nuclei, emitted α particles or fission products, and detector resolution. Recording the data event by event allows for the analysis of delayed coincidences with variable position and time windows for the identification of the decay chains.

This method was developed and tested in experiments investigating neutron-deficient α emitters and proton radioactivity near $N=82$ (Hofmann *et al.*, 1979). The detector system was enlarged, and an array of seven position-sensitive silicon detectors (Hofmann *et al.*, 1984) was used in the identification of the elements bohrium, hassium, and meitnerium (Münzenberg, 1988). An even larger system was built at SHIP in order to search for the elements beyond meitnerium (Hofmann, 1994).

The new detector system is composed of three time-of-flight detectors, seven identical 16-strip silicon wafers, and three germanium detectors. A three-dimensional view of the detector arrangement is shown in Fig. 2, together with a cross section drawn to scale. In front of the silicon detectors, there is a mechanism for changing the calibration sources and degrader foils. The thickness

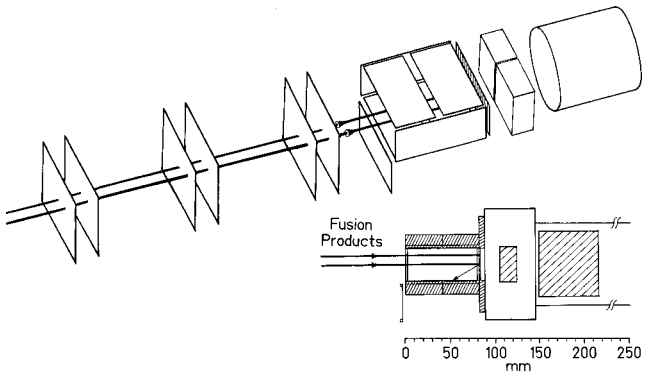

FIG. 2. Assembly of detectors for identification of heavy elements, composed of large-area secondary-electron time-of-flight detectors, position-sensitive silicon strip detectors, and germanium detectors (see text for details).

of the foils (Mylar) can be varied in increments of 0.5 μm in order to facilitate the absorption of low-energy projectiles and reduce the implantation energy, thus avoiding tails on the signals.

The active area of each silicon wafer is $35\times80\,\mathrm{mm}^2$. Each strip is 5 mm wide and position sensitive in the vertical direction with a relative resolution of 150 μm full width at half maximum (FWHM) for the α decays of a decay chain. For that reason, the stop detector is equivalent to 3700 single detectors, each with a 100% active area of $0.15\times5\,\mathrm{mm}^2$. The energy resolution is 14 keV for α particles from a ^{241}Am source or α decays of implanted nuclei. Six wafers are mounted in the back hemisphere facing the stop detector. They measure escaping α particles or fission fragments with a solid angle of 80% of 2π. In the case of the back detectors, neighboring strips are connected galvanically, forming 28 energy-sensitive segments. The direction of the escaping α particle or fission fragment can be roughly retraced. The energy resolution obtained by summing the energy-loss signal from the stop detector and the residual energy from the back detector is 40 keV for α particles. All silicon detectors are cooled to 263 K.

Lifetimes as short as 15 μs are measured with ideal position and energy resolution using fast analog-to-digital converters (3.5 μs conversion time) and 128-word FIFO first-in first-out buffers in each channel. The widths of the signals are determined by the shaping-time constants of 0.3 μs for the position signals and 2.0 μs for the energy signals, which are obtained by summing the two preamplifier signals of each individual strip. The shorter shaped position signals are also used to obtain the energy information for the 3–15 μs range. If two events appear within 15 μs, the second event signals (energy, position, time-to-amplitude converter signal) are shifted out of the dead time of the first event by a constant delay of 50 μs.

The germanium detectors measure x rays or gamma rays that are coincident within a time window of 4 μs with signals from the silicon detectors. This allows for the detection of α transitions to excited levels in the daughter nucleus, which decay by gamma emission. In the case of an electron conversion process, characteristic x rays may be emitted, which would allow for a clear element identification. Although the probability for detecting coincident events is small, the germanium detectors provide useful spectroscopic information if the cross sections are of the order of nanobarns or higher.

In front of the silicon detectors and degrader stack, there are three secondary-electron foil detectors mounted 150 mm apart from each other (Śaro *et al.*, 1996). Two foils made of 30-$\mu g/\mathrm{cm}^2$-thick carbon are needed for each detector. Between the foils an electric potential of ≈4 kV is applied in order to accelerate electrons emitted from the first foil when a heavy ion passes through. Perpendicularly, a magnetic field is applied in order to bend the electrons onto a channel plate for further amplification. The foils are self-supporting and the transmission is 100%. The detector signals are used to distinguish implantation from radioactive decays of previously implanted nuclei. Three detectors are used to increase detection efficiency. Because of the high efficiency of each of these detectors, the background due to projectiles in the decay spectra is suppressed by a factor of a thousand, and the time window for measuring generic parent-daughter decays is significantly prolonged. The time resolution of the foil detectors is about 700 ps and small enough that, taking the energy signals from the silicon detector into account, a rough mass assignment with an accuracy of $\pm10\%$ for the implanted ions is achievable.

The establishment of a generic link of signals from radioactive decays to known daughter decays provides a method for unambiguous identification of the unknown parent isotope. Ghiorso *et al.* (1969) originally applied this method when they identified ^{257}Rf and ^{258}Rf by ''milking'' their daughter nuclides, ^{253}No and ^{254}No. In measurements at recoil separators, the event chain starts with the implantation of the produced nuclide. The measured signals deliver time-of-flight, moment, energy, and position of implantation into the silicon detector. In an ideal case, a sequence of signals follows from α decays. From each decay, the time, energy, and position are again measured, but no signal is obtained from the time-of-flight detectors. The chain ends due to fission or long half-life of the decay products. The limiting longest half-lives are determined solely by the background conditions.

III. EXPERIMENTAL RESULTS

A. The new elements 107 to 112

In this section, we present results dealing with the discovery of elements 107 to 112. The history of the discovery of the transuranium elements up to $Z=106$ was described by Flerov and Ter-Akopian (1983) and by Seaborg and Loveland (1990). A detailed presentation and discussion of the decay properties of elements 107 to 109 and of elements 110 to 112 has been given in previous reviews (Münzenberg, 1988; Hofmann, 1998).

The nuclei known at present are shown in the partial chart of nuclides in Fig. 3. The measured total half-lives are indicated.

Bohrium, element 107, was produced and identified unambiguously by Münzenberg *et al.* (1981). It was the first new element synthesized at SHIP using the method of in-flight recoil separation and generic correlation of parent-daughter nuclei. The reaction used was $^{54}Cr+^{209}Bi\rightarrow^{263}107^*$. Five decay chains were observed, initiated by a 10.38-MeV α transition with a half-life of $(4.7^{+2.3}_{-1.6})$ ms, and one with an energy of 9.70 MeV occurring after 165 ms. In three cases, the granddaughter decays could be assigned to ^{254}Lr, in two cases, the decays of further descendants were assigned in the same way to ^{250}Fm, and in one case to ^{250}Md. Therefore the original parent was assigned with high probability to $^{262}107$.

The accuracy of the decay data was improved in a later work (Münzenberg *et al.*, 1989), and the next lighter isotope, ^{261}Bh, was synthesized at a higher beam energy. Additional data were obtained from the α decay of ^{266}Mt (Hofmann *et al.*, 1997), and the isotope ^{264}Bh was identified as the granddaughter in the decay chain of $^{272}111$ (Hofmann *et al.*, 1995b).

In recent conferences, Gäggeler (1999) and Gregorich (1999) reported on the observation of ^{266}Bh and ^{267}Bh, respectively. The isotopes were produced using the reaction $^{22}Ne+^{249}Bk\rightarrow^{271}Bh^*$. The α energies are 9.30 and 8.85 MeV, the half-lives 1 and 17 s, respectively.

Hassium, element 108, was synthesized in 1984 using the reaction $^{58}Fe+^{208}Pb$. The identification was based on the observation of three atoms (Münzenberg, Armbruster, *et al.*, 1984). Only one α-decay chain was measured in the irradiation of ^{207}Pb with ^{58}Fe. This event was assigned to the even-even isotope ^{264}Bh (Münzenberg, Armbruster, *et al.*, 1986). The results were confirmed in a later work (Hofmann *et al.*, 1995a; Hofmann, 1998), and for the decay of ^{264}Hs, a fission branching of 50% was also measured.

The heaviest known isotope of element 108, ^{269}Hs, was discovered as a link in the decay chain of $^{277}112$ (Hofmann *et al.*, 1996; see Figs. 3 and 4). The measured half-lives of the hassium isotopes range from 0.45 ms for the only known even-even isotope ($A=264$) to 9.3 s for the most neutron-rich one. It should be noted that a half-life close to 10 s is unusually long for an element at the limits of the chart of nuclei.

Meitnerium, element 109, was first observed in the year 1982 in the irradiation of ^{209}Bi with ^{58}Fe by a single α-decay chain, which was assigned to the isotope with a mass number $A=266$ (Münzenberg, Armbruster, *et al.*, 1982; Münzenberg, Reisdorf, *et al.*, 1984). This result was later confirmed by the observation of one more decay chain (Münzenberg, Hofmann, *et al.*, 1988). Another chain presented in the 1988 publication is incomplete. It starts with the decay of ^{262}Bh. Possible reasons for the missing link, the decay of ^{266}Mt, were discussed by Münzenberg, Hofmann, *et al.*, (1988). An (αn) channel was excluded due to kinematical reasons. In the most recent experiment (Hofmann *et al.*, 1997), 12 atoms of ^{266}Mt were measured, revealing a complicated decay pattern, as could be concluded from the wide range of α energies from 10.5 to 11.8 MeV. This property seems to be common to many odd and odd-odd nuclides in the region of the heavy elements.

The more neutron-rich isotope ^{268}Mt was discovered in the decay chain of element 111 (Hofmann *et al.*, 1995b). The two known isotopes of element 109, ^{266}Mt and ^{268}Mt, exhibit only α decay; their half-lives are 1.7 and 70 ms, respectively.

Element 110 was discovered in 1994 using the reaction $^{62}Ni+^{208}Pb\rightarrow^{270}110^*$. The main experiment was preceded by a thorough study of the excitation functions for the synthesis of ^{257}Rf and ^{265}Hs in order to determine the optimum beam energy for the production of element 110. The data revealed that the maximum cross section for the synthesis of element 108 was shifted to a lower excitation energy, different from the predictions of reaction theories (see Fig. 18 in Sec. VI.A.).

A total of four decay chains were observed, and they were assigned to the isotope $^{269}110$ (Hofmann *et al.*, 1995a). The isotope $^{271}110$ was synthesized with a beam of the more neutron-rich isotope ^{64}Ni (Hofmann, 1998). The half-lives of the two α-emitting isotopes are (170^{+160}_{-60}) μs and $(1.1^{+0.6}_{-0.3})$ ms, respectively. There is strong evidence suggesting a second transition with a (56^{+270}_{-26})-ms half-life in $^{271}110$. The important result for the production of elements beyond meitnerium was that the production cross section was enhanced from 3.5 to 15 pb (picobarns) by increasing the neutron number of the projectile by 2, which gave hope that the cross sections could decrease less steeply with more neutron-rich projectiles.

Two more isotopes of element 110 have been reported in the literature. The first is $^{267}110$, produced in the irradiation of ^{209}Bi with ^{59}Co (Ghiorso *et al.*, 1995a, 1995b). This result needs to be confirmed because the daughter generations within the only observed decay chain are fairly incomplete. The second isotope is $^{273}110$, reported to be observed in the irradiation of ^{244}Pu with ^{34}S after the evaporation of five neutrons (Lazarev *et al.*, 1995, 1996). The measured data are presented in more detail in Sec. IV.D.2.

Element 111 was synthesized in 1994 using the reaction $^{64}Ni+^{209}Bi\rightarrow^{273}111^*$. A total of three α chains of the isotope $^{272}111$ were observed (Hofmann *et al.*, 1995b). The half-life is $(1.5^{+2.0}_{-0.5})$ ms and the cross section $(3.5^{+4.6}_{-2.3})$ pb.

Element 112 was investigated at SHIP using the reaction $^{70}Zn+^{208}Pb\rightarrow^{278}112^*$ (Hofmann *et al.*, 1996). The irradiation was performed at a beam energy of 344 MeV in January-February 1996. Over a period of 24 days, a total of 3.4×10^{18} projectiles were collected. Two α-decay chains were observed, resulting in a cross section of $(1.0^{+1.3}_{-0.7})$ pb.

The two α-decay chains were assigned to the one neutron-emission channel. The measured half-lives and Q_α values are shown in Fig. 4. Although the data agree well for the α decay of ^{269}Hs and further downwards, the first two decays of chain 1 reveal significant differences

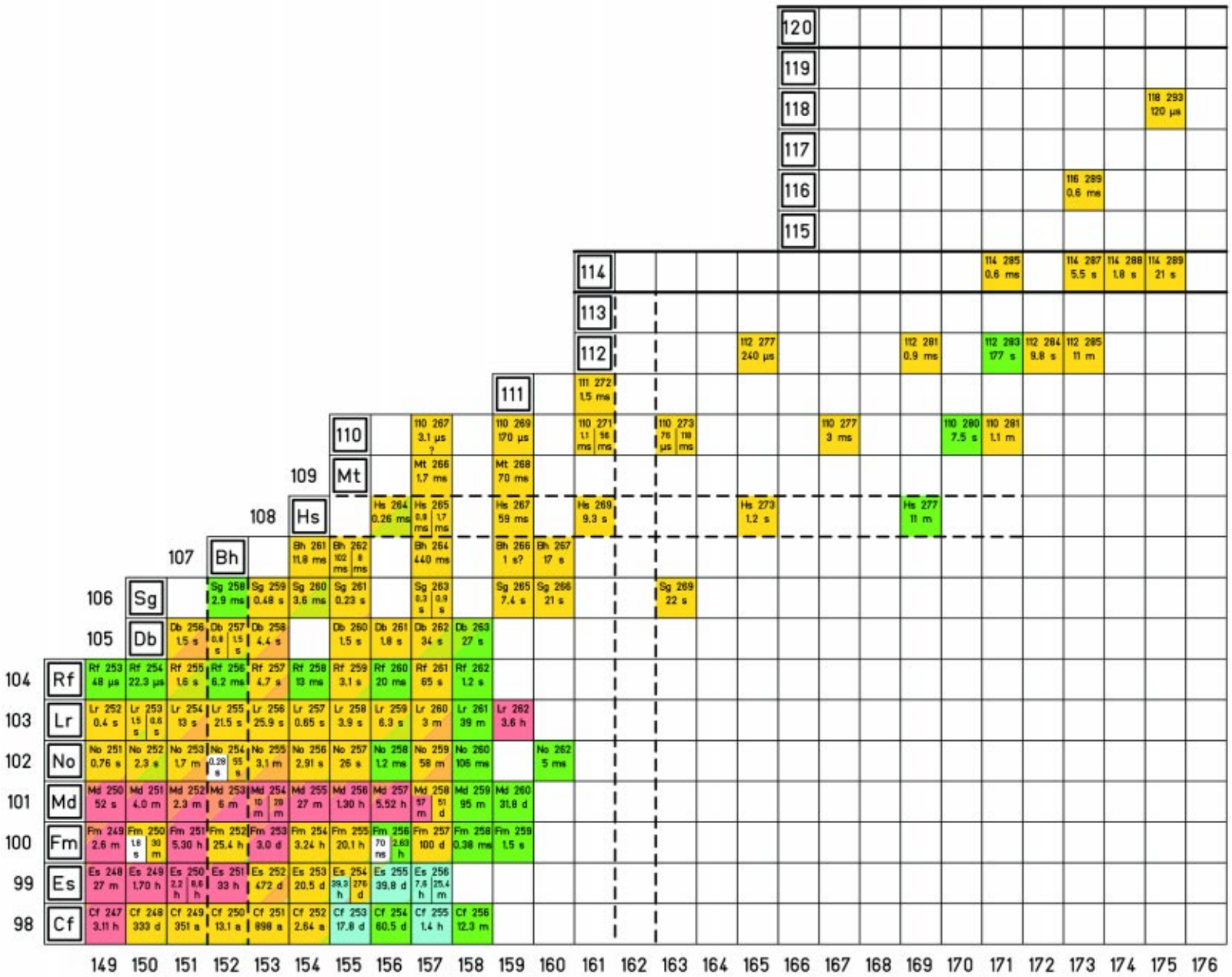

FIG. 3. The upper end of the chart of the nuclides showing the experimentally investigated isotopes. The numbers given are the measured total half-lives. The colors stand for the decay mode; they are the same as the ones used in the chart of nuclides published by Pfenning *et al.* (1998): α decay, yellow; β^+ or electron-capture decay, red; β^- decay, blue; spontaneous fission, green; and isomeric transitions, white. The areas are proportional to the branching ratios [Color].

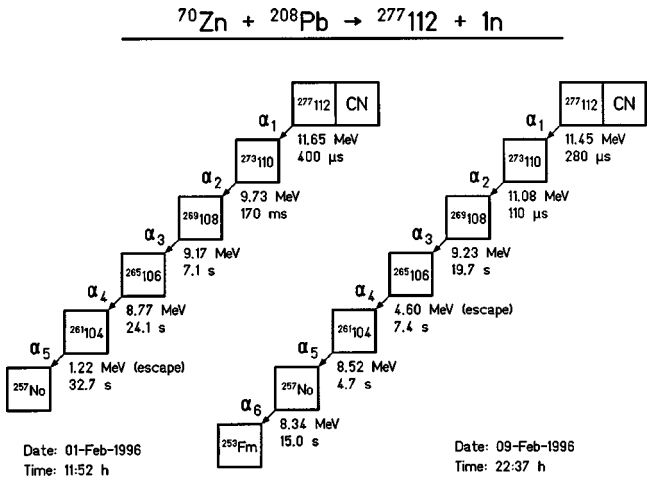

FIG. 4. The α-decay chains of the two atoms of element 112 observed at GSI, Darmstadt. From Hofmann *et al.*, 1996.

compared with the result of chain 2. The measured α energy of $^{273}110$ is lower by 1.35 MeV and the lifetime is 1545 times longer. In view of this great difference in the lifetimes, the two transitions must be assigned to different levels in $^{273}110$. The energies of the two α transitions of $^{277}112$ differ by 200 keV, which is 13 times larger than the energy resolution of the detector. Although the lifetime of the two transitions is similar, the population of the two different levels in $^{273}110$ suggests that two different levels are already populated in $^{277}112$ by the reaction process.

The trend of Q_α values (Fig. 5) shows that the smooth dependence as a function of the neutron number is broken for chain 1, when $N=164$, and for chain 2, when $N=162$ is crossed. Similar irregularities of the Q_α systematics are observed near closed shells, e.g., the Q_α values drop by 2 MeV when the closed neutron shell $N=126$ is crossed. For the two decay chains of $^{277}112$, this could infer a pronounced shell effect at $N=164$ for chain 1 and at $N=162$ for chain 2.

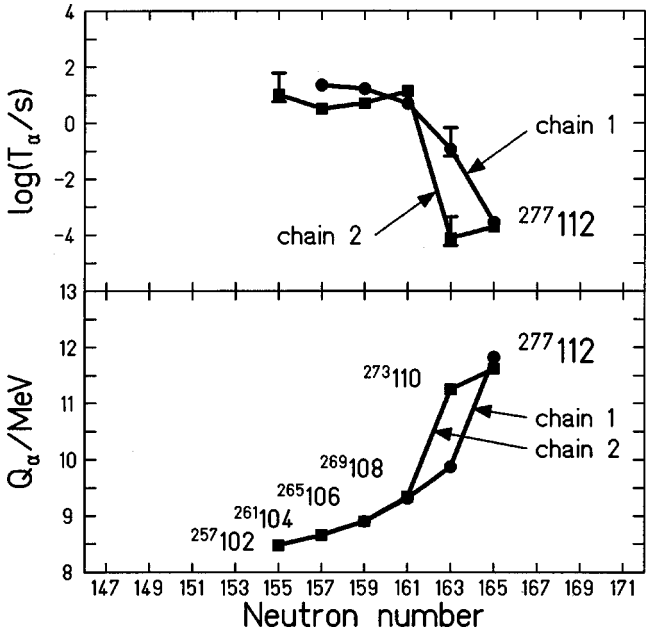

FIG. 5. Systematics of the two decay chains of $^{277}112$: upper part, measured half-lives; lower part, Q_α values. Examples of the error bars of the half-lives are shown in three cases. They reflect the statistical uncertainty in the case of one event.

Theoretical binding-energy calculations (Möller, Nix, *et al.*, 1995a, 1995b; Smolanczuk and Sobiczewski, 1995a, 1995b) predict a minimum in the negative shell-correction energies at neutron number $N=162$ and proton number $Z=108$. It is calculated that the nuclei in that region are strongly deformed, with deformation parameters $\beta_2\approx 0.23$ and $\beta_4\approx -0.08$. The properties of chain 2 are in good agreement with the calculated binding energies of the ground states. Therefore we may conclude that $^{277}112$ of chain 2 was produced in the deformed ground state and that α decay populates the deformed ground state of the daughter nuclei of the decay chain.

A second minimum, but for spherical shapes, was calculated at neutron number $N=164$. It arises at low energy due to the influence of the close-lying spherical shell at $Z=114$. For the case of $^{278}_{164}114$, the calculation predicts an energy difference relative to the deformed ground state of only 300 keV (Möller, Nix, *et al.*, 1995a, 1995b). Therefore, in constructing a working hypothesis, we may assume that chain 1 is produced by the population of a spherically shaped isomer in $^{277}_{165}112$. The α decay populates spherically shaped isomers, which increase in energy relative to the ground states, down to ^{269}Hs, where the transition to the deformed ground state occurs by γ emission. The width of the γ transition would only be visible in the experiment if it were narrower than the width of the ^{269}Hs α decay, which has a half-life of approximately 10 s.

The interpretation presented here is speculative and hence not the only possible one. Another explanation might be found by taking spin isomerism into account. In this region of nuclei, isomerism is a characteristic feature of odd nuclei. Isomerism has been observed in ^{263}Sg, ^{262}Bh, ^{265}Hs, $^{271}110$, and $^{273}110$. Although a definitive assignment is not possible on the basis of the sparse data now available, theoretical investigations show that spin isomerism is highly probable in odd-neutron nuclei (Ćwiok *et al.*, 1994). Their existence is closely associated with the bunching of levels of spin values from 1/2 to 13/2 at neutron number $N=162$ for deformed nuclei. The anomalous behavior noted in the case of the decay of $^{273}110$ is related to the extremely large energy difference of 1.35 MeV measured between the two α decays.

B. Neutron-deficient isotopes and the $N=152$ shell effect

The decay properties of neutron-deficient isotopes of the heavy elements are influenced by the increasing probability of spontaneous fission (see Figs. 16 and 17 in Sec. V.B). Beta-delayed fission or fission of the ground states or isomeric states are expected with decreasing half-lives.

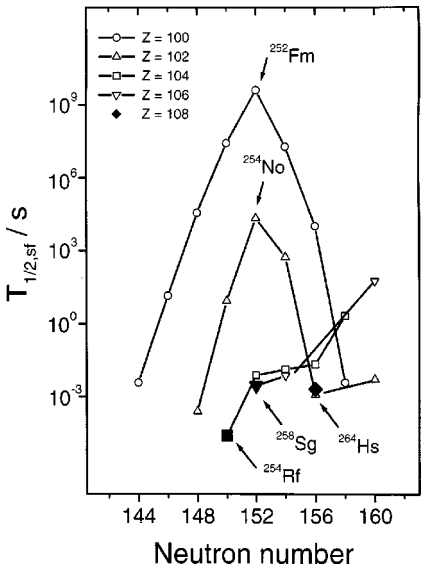

FIG. 6. Plot of fission half-lives of even-even nuclei. The new data (Heßberger *et al.*, 1997) are marked by filled symbols.

The fission barriers are strongly modulated by shell-correction energies. Extended fission half-lives at neutron number $N=152$, due to a gap in the neutron single-particle energy levels, have been recognized (Ghiorso, 1970). The decline of the fission half-lives by seven orders of magnitude from ^{254}No ($T_{1/2,sf}=2.2\times10^4$ s; Türler *et al.*, 1988) to ^{256}Rf ($T_{1/2,sf}\approx5$ ms; Oganessian, Iljinov, *et al.*, 1975) could be explained by a lowering of the outer second hump of the fission barrier below the ground-state energy. As a result, the width of the fission barrier is strongly reduced.

In order to confirm the stabilizing shell effect at $N=152$, the isotopes ^{254}Rf and ^{258}Sg were investigated at SHIP. Corresponding half-lives of $T_{1/2,sf}=(23\pm3)$ μs and $T_{1/2,sf}=(2.9^{+1.3}_{-0.7})$ ms were measured (Heßberger *et al.*, 1997). The extended systematics of fission half-lives (Fig. 6) is clear evidence of an increased shell effect at $N=152$ up to seaborgium.

Besides the investigation of even-even nuclei, the new isotope ^{253}Rf, $T_{1/2,sf}=(48^{+17}_{-10})$ μs, was identified and more detailed α-spectroscopic data on isotopes ^{255}Rf and ^{257}Rf were obtained (Heßberger *et al.*, 1997). In reactions of ^{40}Ar with ^{209}Bi targets, new isotopes of mendelevium (^{246}Md, ^{247}Md) and einsteinium (^{242}Es, ^{241}Es) were synthesized (Ninov *et al.*, 1996). These isotopes are dominantly α emitters, with the exception of a relatively short-lived fission activity of $T_{1/2,sf}=(0.90\pm0.25)$ ms, which was tentatively assigned to the ground state of ^{245}Md. For the ground state, a spin and parity of $1/2^-$ was considered, whereas the α activity was expected to be emitted from a $7/2^-$ or $7/2^+$ isomeric state.

C. Neutron-rich isotopes and the bimodal fission

Rapid changes in the fission properties of heavy elements are grounds for excitement and intensive work, both experimentally and theoretically. This was the case

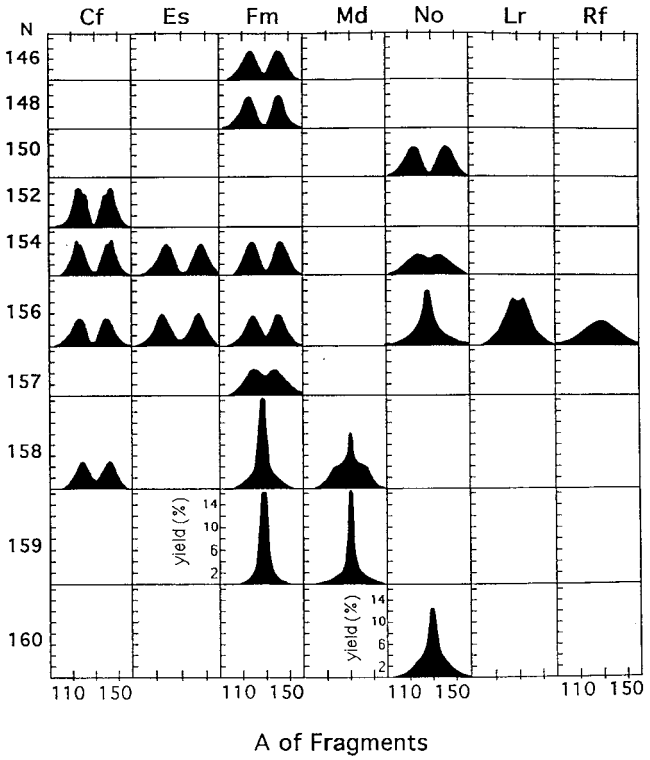

FIG. 7. Schematic representation of mass yield distributions (normalized to 200% fission fragment yield) for the spontaneous fission of isotopes of californium to rutherfordium. From Hofmann, 1994.

when the short fission half-life of ^{256}Rf was measured in experiments in Dubna (Oganessian, Iljinov, *et al.*, 1975; see previous section). Another case of rapid changes was observed in the region of heavy fermium isotopes in the 1970s. The first observation of the onset of symmetric fission was made in a study of ^{257}Fm (Balagna *et al.*, 1971). For ^{258}Fm, the changes are even more dramatic. Fission becomes symmetric, with a very narrow mass distribution. The kinetic energy of the fragments is about 35 MeV higher than that in the asymmetric fission of ^{256}Fm, and the spontaneous fission half-life is 0.38 ms, compared with 2.63 h for ^{256}Fm. Other cases of symmetric fission are summarized in Fig. 7.

An important feature of some of the kinetic energy distributions is that they do not assume a Gaussian shape. Instead, some of the distributions are best described as a sum of two Gaussians (Hulet *et al.*, 1986). This type of fission is referred to as "bimodal" fission.

It has been proposed that the rapid change in half-life when going from ^{256}Fm to ^{258}Fm results from the disappearance of the second saddle in the barrier below the ground-state energy, in the same manner as for ^{256}Rf. However, theoretical studies have presented another explanation (Wilkins *et al.*, 1976; Ćwiok *et al.*, 1989; Möller *et al.*, 1989).

The paths of the bimodal fissioning nucleus ^{258}Fm on the potential-energy surface are shown in Fig. 8. Initially, there is only one path starting at the ground state. Later, it divides into two paths, one leading to compact scission shapes with high kinetic energy, and the other

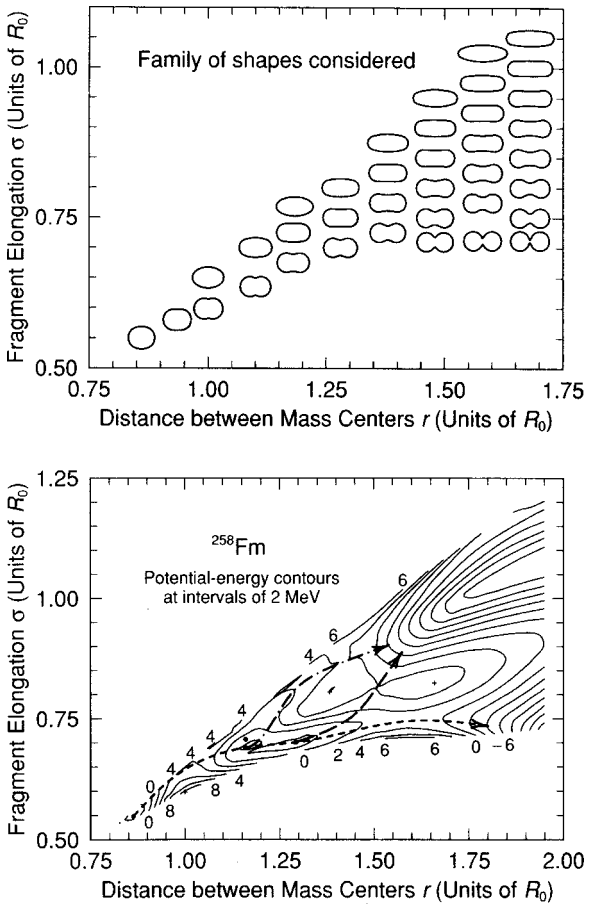

FIG. 8. Fission paths for the explanation of the bimodal fission of ^{258}Fm: upper part, nuclear shapes for which potential-energy surfaces were calculated; lower part, potential-energy surface calculated at intervals of 2 MeV. R_0 is the spherical nuclear radius. From Möller and Nix, 1992.

leading to elongated shapes with normal kinetic energies. At a later stage in the barrier penetration process, a third switchback path branches off from the path leading to compact shapes and leads back into the valley of elongated scission shapes. The inertia associated with fission into the lower valley is considerably smaller than the inertia for fission into the upper valley. This is the reason for the short fission half-life of ^{258}Fm.

The compact scission shapes develop close to the fragment magic numbers $Z_{1,2}=50$ and $N_{1,2}=82$ and disappear far away from these numbers. Thus the shortest half-lives along the symmetric fission valley are expected for $^{264}_{100}\mathrm{Fm}_{164}$. The effect of fragment shells at a relatively early stage of the fission process was brought up in the mid 1970s (Maruhn and Greiner, 1974; Wilkins *et al.*, 1976).

Möller and Nix (1992) pointed out the balance between the stabilizing effect of neutron number $N=162$ on the ground state of elements near $Z=110$ and the destabilizing effect of $N=164=2\times82$, which differs by only two neutron numbers. In this case, however, the measured α decay of the new elements 110 to 112 and of their daughter nuclei with relatively long half-lives proved the stabilizing effect to be stronger, probably due to the vanishing fragment shell effects at a distance from $Z=100$.

In general, fission and fusion are not reversible processes. Asymmetric fission along the elongated path is associated with relatively high excitation of the fragments, neutron evaporation, and neck formation. However, compact symmetric fission is a reversible process. The inertia is small, the fragments are less excited, and fewer or even no neutrons are emitted. In analogy to cold fusion, we speak of cold fission. The importance of cold processes for fusion, including symmetric systems, was pointed out quite early by Săndulescu *et al.* (1976). However, the proposed reaction $^{134}\mathrm{Xe}+^{124}\mathrm{Sn}\rightarrow^{258}\mathrm{Rf}^*$ is still awaiting experimental proof.

D. Ground-state band and deformation of ^{254}No

Two problems remaining unanswered were recently tackled experimentally: What is the maximum angular momentum that heavy nuclei can bear during the formation process, and what is the degree of deformation in the ground state? The observation of high-spin states ($I\geqslant10$) gives information on the fission barrier of heavy nuclei at high angular momentum. This information is important for understanding the mechanism of the synthesis, since the fission barrier governs the survival probability. In fact, it is *a priori* not obvious that high-spin states of shell-stabilized nuclei will even survive against fission. Secondly, the stability of the isotopes that have so far been discovered of elements beyond fermium is predicted to arise from the ability of the nucleus to deform. However, a direct proof and a measurement of the degree of deformation were still missing.

The standard method for identifying high-spin states is in-beam γ spectroscopy, but it is rarely used for studying very heavy nuclei because of an overwhelming fission background. This problem was overcome by Reiter *et al.* (1999) in an experiment in July, 1998, at the Argonne superconducting linear accelerator ATLAS by combining highly efficient detectors and selecting a reaction with the highest known cross section for the production of a transfermium nucleus.

Reiter *et al.* (1999) investigated the reaction $^{48}\mathrm{Ca}+^{208}\mathrm{Pb}\rightarrow^{254}\mathrm{No}+2\mathrm{n}$, which has a cross section of 3 μb. The γ rays were detected using the Gammasphere, consisting of 101 Ge detectors. In order to identify γ rays from ^{254}No in a background of more than 10^4 times more intense fission γ rays, it was essential to require coincidences with evaporation residues. These were separated in flight within 10^{-6} s from the beam by the fragment mass analyzer (FMA; Davids, 1992). At the focal plane of the FMA, particles passed through transmission detectors and were then implanted into a position-sensitive double-sided Si-strip detector, which had 1600 1×1-mm pixels. The production of ^{254}No was unambiguously demonstrated by the observed α decay, which occurred with a half-life of 55 s in the same pixel of the detector where the nucleus had been implanted. The γ spectrum, tagged in this way, shows the nobelium K_α and K_β x rays, and a sequence of transitions with

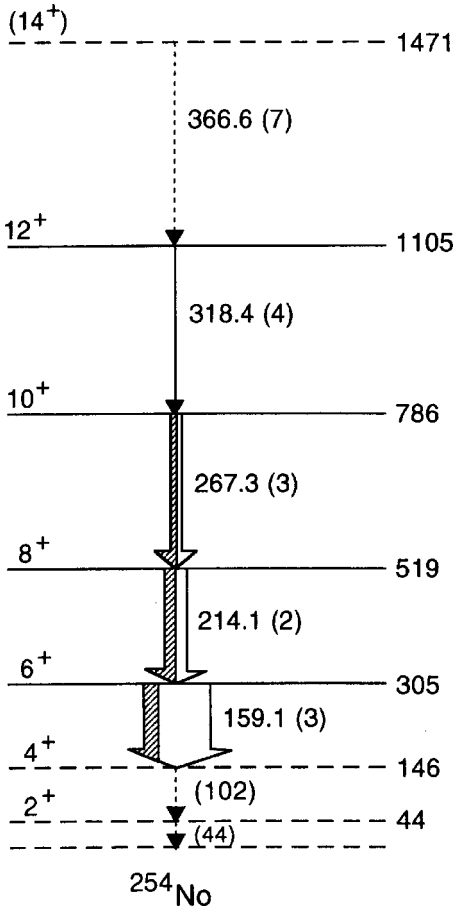

FIG. 9. Proposed level scheme for the ground-state band of ^{254}No. From Reiter *et al.*, 1999.

spacings that are characteristic of transitions from a rotational band of a deformed nucleus.

A total of four γ lines were identified and assigned to a cascade of electric quadrupole transitions ($E2$), starting from a level of spin and parity 12^+ (Fig. 9). The two lowest of the six possible transitions were not observed because they decay almost entirely by conversion. From the energies of the transitions, a quadrupole deformation parameter $\beta_2 = 0.27 \pm 0.02$ was deduced, which is in excellent agreement with theoretical predictions (Patyk and Sobiczewski, 1991; Ćwiok *et al.*, 1994, 1996; Möller *et al.*, 1995a 1995b; Lalazissis *et al.*, 1996; Rutz *et al.*, 1997). The nucleus ^{254}No is a prolate spheroid with an axis ratio of 4:3.

The energies of the rotational levels 2^+ and 4^+ were estimated as (44 ± 1) keV and (102 ± 1) keV using energy-spin relationships. The energy of the 2^+ state is in good agreement with calculations by Muntian *et al.* (1999). They obtained for shell-stabilized nuclei (at $N = 152$) a minimum rotational energy of 41.7 keV for ^{254}No and at $N = 162$ a minimum of 40.0 keV for ^{270}Hs.

One month after the experiment at Argonne, in August, 1998, the experiment was repeated at the cyclotron of the University of Jyväskylä, Finland (Leino *et al.*, 1999). There the detectors were arranged before and behind the gas-filled separator RITU (Leino, 1994). In this experiment, a tentatively assigned transition $14^+ \rightarrow 12^+$ observed in the Argonne experiment was confirmed, and a new transition, probably $16^+ \rightarrow 14^+$, was added.

The observation of states with spin up to 16 implies that neutron evaporation can partially compete against fission up to at least that spin. Hence a fission barrier must still exist up to that angular momentum and corresponding excitation energy in ^{254}No. In their future work, the groups plan to investigate the fission barrier and its dependence on angular momentum. The measurements will also yield important information regarding the original spin distribution, which will provide more insight into the production mechanism of the heaviest elements.

IV. EXPLORATION OF THE ISLAND OF SUPERHEAVY ELEMENTS

Shell effects *per se* mark discontinuities in the trend of atomic and nuclear properties. As a result, lifetimes, cross sections, and other properties may be modulated in an unforeseeable way. Therefore the exploration of new regions that are expected to be dominated by shell effects demands and justifies investigations for which the result is not predictable. In these cases, even negative results are valuable, if experimental flaws can be excluded. In other cases, we may obtain results that cannot be explained immediately but that are important enough to pursue with additional efforts. In the following sections, we present some recent experiments performed at GSI, Darmstadt, with negative results, as well as at JINR, Dubna, and LBNL, Berkeley, with exciting results that, if confirmed, will be a breakthrough in superheavy element research.

A. Search for ^{275}112

The measured cross section for the production of ^{277}112 using the reaction ^{70}Zn+^{208}Pb was 1 pb. This value is smaller than the extrapolated value of 3 pb based on cross-section trend. Still, the statistical uncertainty of the measured value does not challenge the higher value of the extrapolation. The reason for this difference could also be that the beam energy was not chosen in accordance with the maximum production cross section.

Moreover, a cross section ''inversion'' as a function of isospin may occur in the case of element 112 isotopes if the shell-correction energies of the fusion products influence the production probabilities. At lower (negative) shell-correction energies, the fission barrier of the relatively cold compound nucleus is higher and wider, resulting in higher survival probability. The isotopes ^{273,275}112, which may be produced using ^{66,68}Zn beams, are predicted to be more strongly bound than ^{277}112, which results from the use of a ^{70}Zn beam [Fig. 10(b)]. In the case of $Z = 110$ isotopes, the cross section increased by a factor of 4.3 as the projectile beam was changed from ^{62}Ni to ^{64}Ni [Fig. 10(a)]. Whether or not this increase in cross section is mainly attributable to the lower shell-correction energy can be verified with stable

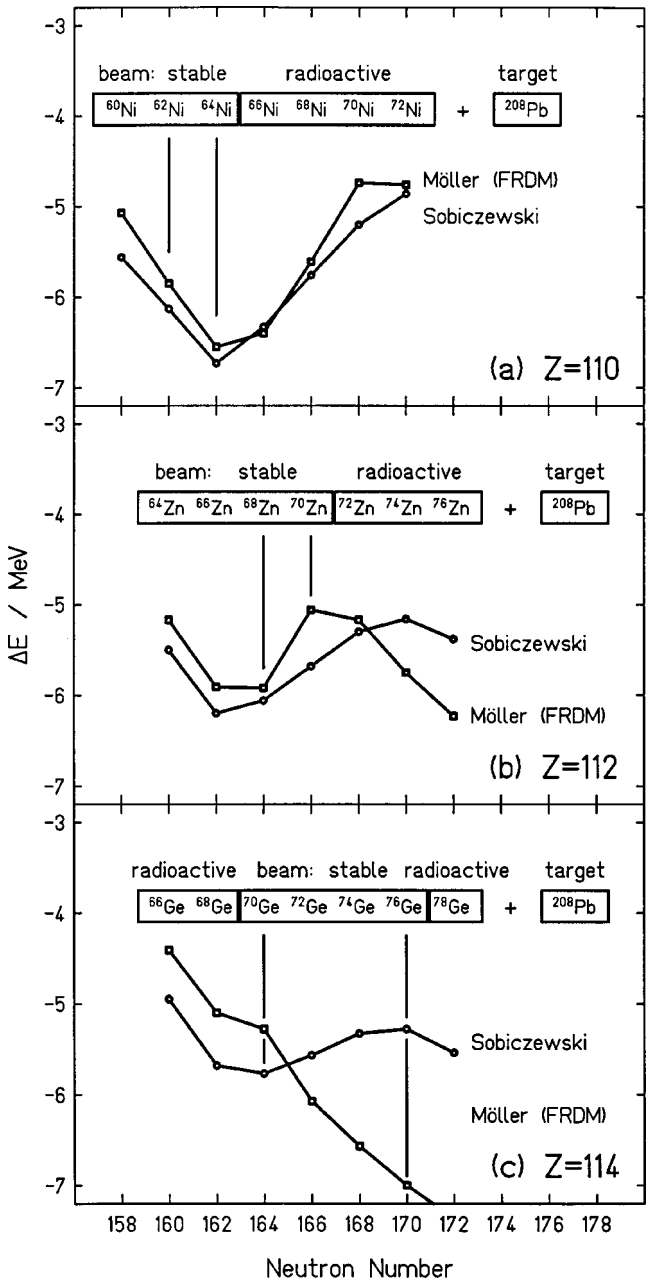

FIG. 10. Calculated shell-correction energies from Sobiczewski (1994) and Möller and Nix (1994): (a) for isotopes of $Z=110$; (b) for isotopes of $Z=112$; and (c) for isotopes of $Z=114$. A possible correlation with cross sections could be tested in the case of element 112 with stable projectiles of ^{66,68,70}Zn. The monotonic decrease of the data calculated by Möller and Nix in (c) is due to the spherical shell closure of superheavy elements at $Z=114$ and $N=184$, whereas the minimum in (a) and (b) is due to a large level spacing at $N=162$ for deformed nuclei.

projectiles in the case of $Z=112$ isotopes. The neutron-rich zinc beams make the crossing of the neutron number $N=162$ possible for the first time in lead-based reactions.

A search experiment for ^{275}112 via the reaction ^{68}Zn+^{208}Pb was performed in March-April, 1997, at SHIP. At two different beam energies, cross-section limits of 1.2 pb were reached. The attained limits do not exclude a cross section comparable to the 1 pb measured for ^{277}112 with a ^{70}Zn beam; however, they do exclude a cross-section increase by a factor greater than 3, due in part to shell effects at neutron numbers close to $N=162$. This result favors the use of a ^{70}Zn beam in the production of element 113.

Figure 10(c) shows that the predictions diverge as the distance from the region of known isotopes increases and when the region of spherical SHE's is entered. The uncertainty of the calculations rises up to values of $\approx$1.7 MeV in the case of ^{284}114. A low, negative shell-correction energy would increase the half-life of the isotope in the ground state and could also influence the production cross section significantly.

B. Search for element 116 and the radiative-capture channel

A close approach to the region of spherical SHE's using ^{208}Pb targets is possible with ^{82}Se projectiles. In that reaction, the ^{290}116 nucleus may be produced by a radiative capture process. The predicted shell correction energies are -6.1 MeV (Smolanczuk and Sobiczewski, 1995a, 1995b) or -7.8 MeV (Möller *et al.*, 1995a, 1995b). For comparison, minimum shell-correction energies in the region of SHE's were calculated for ^{296}114 (-7.2 MeV) and for ^{294}115 (-9.4 MeV) by Smolanczuk and Sobiczewski (1995a, 1995b) and by Möller *et al.* (1995a, 1995b), respectively.

Half-life calculations propose an α-decay chain of six decays from ^{290}116 down to ^{266}Rf (Möller *et al.*, 1995a, 1995b; Smolanczuk and Sobiczewski, 1995a, 1995b). The half-life values range from milliseconds to several seconds for the first five decays and from 50 s to 0.4 h for ^{270}Sg. The latter isotope may already have ended the chain by fission. A partial fission half-life of 55 s was calculated by Smolanczuk *et al.* (1995). The chain will most likely end by fission of ^{266}Rf. A calculated fission half-life is 23 s and a calculated α branching is only $\approx 10^{-5}$. All isotopes of the decay chain would be new. However, the properties of the chain would be unique for the decay of a superheavy nucleus, and the predicted half-lives would prove ideal for identification by correlation methods.

The energy needed to reach the contact point of the outer nucleon orbitals seems to be a reliable guide in the estimation of the projectile energy needed to fuse the system ^{82}Se+^{208}Pb. This tendency is suggested by the measured excitation functions for cold-fusion reactions of elements 104 to 110 (see Sec. VI.A, Fig. 18). The needed energy can be calculated using a Woods-Saxon potential. The projectile energy is then determined from the Coulomb potential. The resulting values for the reaction ^{82}Se+^{208}Pb are 14.15 fm for the distance between the centers of the projectile and target nucleus and $E_{CM}=283.0$ MeV for the center-of-mass energy. At this energy, the excitation energy of the fused system will be 4.0 MeV, based on the binding energy of ^{290}116 given by Myers and Świątecki (1996). This value of the excitation

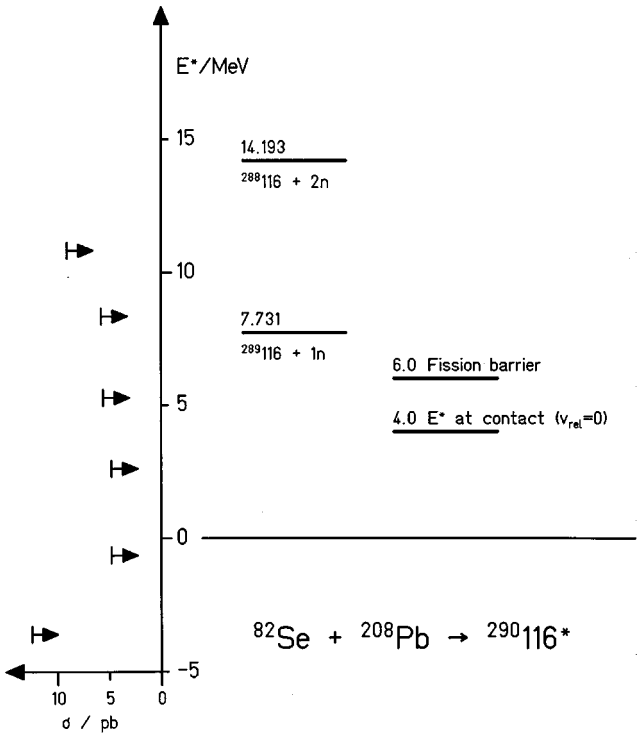

FIG. 11. Cross-section limits reached for the production of $^{290}116$ by the reaction $^{82}Se+^{208}Pb$. The data are compared with the predicted neutron-binding energies, fission barrier, and free reaction energy at the contact point.

energy is smaller than that of the fission barrier. If the system does not undergo separation during the fusion process, the likelihood that the final product will deexcite by γ emission could be relatively high. Level-density arguments demand a higher excitation energy for an increase in the fusion probability. An ideal value is probably at or just below the height of the fission barrier, which, however, remains uncertain for spherical superheavy nuclei. Values close to 6 MeV are predicted by theory (Möller *et al.*, 1995a, 1995b; Smolanczuk and Sobiczewski, 1995a, 1995b).

The irradiation to search for $^{290}116$, produced by radiative capture of ^{82}Se and ^{208}Pb, was completed in November-December, 1995, at SHIP. A summary of the obtained cross-section limits is shown in Fig. 11. In the figure, the investigated range of excitation energies is compared with the neutron-binding energies, the predicted fission barrier, and the energy at the contact point. These calculated values are rather uncertain. Therefore beam energies were chosen over a wide energy range, including even values that would produce the predicted negative excitation energies.

The experiment precludes the fact that the radiative capture channel has an unusually high fusion cross section at extremely low free-reaction energies. Nevertheless, as will be shortly discussed, this channel presents an option for future experiments aiming at synthesizing SHE's.

C. Search for element 113

The successful synthesis of element $Z=113$ would be another step toward the discovery of spherical superheavy nuclei. However, the search for element 113 has been complicated by the fact that, up until recently, no excitation function for the production of odd elements from dubnium ($Z=105$) to element 111 was known well enough to allow for an estimate of the optimum beam energy. Therefore the two reactions $^{50}Ti+^{209}Bi\rightarrow^{259}Db^*$ and $^{58}Fe+^{209}Bi\rightarrow^{267}Mt^*$ were investigated before the main experiment (Hofmann *et al.*, 1997). The most important outcome was that the position and width of the excitation function of the $1n$ to $3n$ channel for dubnium and of the $1n$ channel for meitnerium are the same as for the next lighter even element. Moreover, the alternative of using a zinc beam of projectile mass $A=68$ or 70 was clarified before the main experiment (see Sec. IV.A).

The excitation energy of the compound nucleus for the synthesis of element 112 was 9.85 MeV. The same excitation energy for the production of element 113 is obtained at a beam energy of 348 MeV. Using this energy, the irradiation at SHIP started on March 5, 1998. Targets of ^{209}Bi with 450 $\mu g/cm^2$ thickness were irradiated with ^{70}Zn ions. Within a period of 25 days, a dose of 4.5×10^{18} projectiles was collected. In a second period of 21 days starting on April 15, 1998, the accumulated dose was 3.0×10^{18}. A slightly higher beam energy of 350 MeV was used in the second part of the experiment, resulting in an excitation energy of 11.57 MeV. The beam energy was increased slightly in order to take into account a possible shift of the excitation function to a higher energy, which was indicated by the two data points measured for element 111, although with a low statistical significance. The cross-section limits were 0.9 and 1.4 pb, obtained in the first and second part of the experiment, respectively. The 1.7-MeV step in the excitation energy is small compared to the expected width of the excitation function. Therefore the two limits can still be averaged. A value of 0.6 pb is thus obtained at a weighted mean excitation energy of 10.54 MeV. The cross-section limits are calculated at a confidence level of 68%.

The obtained cross-section limit for synthesizing element 113 is not contradictory to the expectations (see Sec. VI.A, Fig. 19). The limit is still higher than the lower value of the possible range estimated to be within 0.3–1.0 pb. However, we also have to take into account the 1-pb value measured for element 112, for which a maximum value of 3 pb was expected. Then, taking the negative result for element 113 into account, it appears that the production of heavy elements near $^{278}112$ using cold fusion does not profit from the higher isospin value of the ^{70}Zn beam. This was the case in the $Z=110$ experiment when the beam was changed from ^{62}Ni to ^{64}Ni. The experiment also revealed that, with our current experimental setup, the measuring time increases unac-

ceptably for regular investigations with cross sections of the order of a few hundred femtobarns.

D. Synthesis of elements 112 and 114 at U-400 in Dubna

Cold-fusion experiments using targets of lead and bismuth were first performed at the U-400 cyclotron in Dubna. Significant results were obtained in several experiments, up to the investigation of element 109 (Flerov and Ter-Akopian, 1983; Oganessian, Tretyakov, *et al.*, 1974; Oganessian, Hussonnois, *et al.*, 1984). The strategy of the Dubna group was later changed, and the investigation of hot fusion using actinide targets was resumed (Oganessian, 1995). The main arguments for the change resided first in the low cross sections expected for the production of SHE's by cold fusion, due to increasing Coulomb repulsion, and second in the fact that only actinide targets allowed for the production of longer-lived, more neutron-rich nuclei, which are closer to the region of spherical SHE's.

The lowest excitation energies of compound nuclei from fusion with actinide targets are obtained with beams of ^{48}Ca. Due to the high neutron number of ^{48}Ca, the most neutron-rich nuclei can also be reached. The development of an intense ^{48}Ca beam at low consumption of material in the ion source was the aim of the work accomplished in Dubna during a period of about two years until 1998 (Kutner *et al.*, 1998).

The U-400 cyclotron was modified to allow for an axial injection of the beam from an electron cyclotron resonance ion source. The charge state 5^+ extracted from the source allowed for continuous operation of the cyclotron. The beam intensity was increased by a factor of 2–3 over that of the previously used pulsed mode. As a result of the improvements, an intensity at the target of 0.3 p μA of ^{48}Ca was reached at a consumption rate of only 0.3 mg/h. The beam energy was determined and controlled during irradiation with a precision of about ± 1 MeV.

The experiments at the U-400 cyclotron were performed at two different recoil separators, which had been built during the 1980s. The separators had been upgraded in order to improve the background suppression and detector efficiency. The energy-dispersive electrostatic separator VASSILISSA was equipped with an additional deflection magnet (Yeremin *et al.*, 1994, 1997). The gas-filled separator GNS (''Gaso Napolnennyj Separator,'' the Russian expression for gas-filled separator) was tuned for the use of very asymmetric reactions with an emphasis on the irradiation of highly radioactive targets (Lazarev *et al.*, 1993). Both separators were equipped with time-of-flight detectors and with an array of position-sensitive Si detectors in an arrangement similar to the one shown in Fig. 2.

1. Experiments at the electromagnetic separator VASSILISSA

The performance of the separator VASSILISSA was tested in a series of experiments aiming at the identification of new neutron-deficient isotopes of uranium, neptunium, and plutonium (Andreyev *et al.*, 1992a, 1992b, 1993). Hot-fusion reactions leading to the compound nuclei ^{258}No and ^{263}Db were studied (Andreyev *et al.*, 1992a 1992b).

Finally, attempts were undertaken to search for new isotopes of element 112 by irradiation of ^{238}U with ^{48}Ca ions (Oganessian, Yeremin, Gulbekian, *et al.*, 1999). The irradiation started in March, 1998. During a period of 25 days, a beam dose of 3.5×10^{18} projectiles was collected, and during a succeeding period of 15 days, a dose of 2.2×10^{18} was collected. The beam energies were 231 and 238 MeV, respectively, resulting in excitation energies of 33 and 39 MeV. Two fission events were measured at the lower beam energy. The mean half-life was (81^{+147}_{-32}) s and the cross section $(5.0^{+6.3}_{-3.2})$ pb. The two events were tentatively assigned to the residue ^{283}112 after $3n$ evaporation. At the higher beam energy, no events from the decay of heavy nuclei were observed. The cross-section limit reached was 7.3 pb.

The experiments at VASSILISSA were continued in March 1999. The reaction ^{48}Ca+^{242}Pu$\rightarrow^{290}$114* was investigated (Oganessian, Yeremin, Popeko, *et al.*, 1999). It was expected that, after the evaporation of three neutrons, the nuclide ^{287}114 would be produced and would decay by α emission into the previously investigated ^{283}112. Over a period of 21 days, a total of 7.5×10^{18} projectiles were collected. The beam energy was determined so that in the middle of the target thickness a value of 235 MeV was obtained, which corresponds to an excitation energy of the compound nucleus of 33.5 MeV.

A total of four fission events were detected. Two of them could be assigned to fission isomers, tentatively to the 24-μs ^{241mf}Pu, produced by neutron transfer. These two fission signals were registered 59 μs and 20 μs after implantation. The other two fission signals were preceded by signals from α particles (one was an escape α of 2.31 MeV) and implantations. These two chains are displayed in Fig. 12(a). The measured values for energies and lifetimes are also indicated. A cross section of $(2.5^{+3.3}_{-1.6})$ pb was obtained for the two events. They were assigned to the nuclide ^{287}114.

The four events, two from 112 and two from 114 of the ^{238}U and ^{242}Pu irradiation with ^{48}Ca, are consistent. The fission lifetimes are within the limits given by statistical fluctuations. Fission was measured again after α decay, when the target was changed from ^{238}U to ^{242}Pu. The low background rate in the focal plane of VASSILISSA makes a production by chance coincidences unlikely. The excitation energy of 33 MeV is ideal for the evaporation of three neutrons. However, it also allows for the emission of an α particle or a proton. Although the evaporation of charged particles is highly hindered by the Coulomb barrier, this possibility cannot be completely excluded.

The separator VASSILISSA is being further upgraded at present. The last dipole magnet is being replaced by a magnet of higher bending power, with a deflection angle of 37°, which will result in a mass resolution of about 1.5%. This additional information will

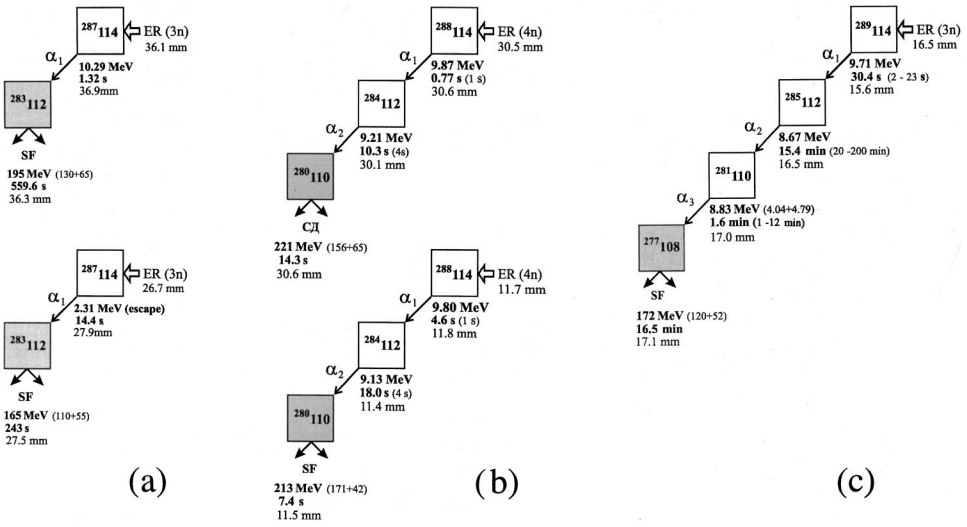

FIG. 12. Decay chains and assignments obtained in experiments at Dubna using the reactions (a) $^{48}Ca+^{242}Pu\rightarrow^{287}114+3n$; (b) $^{48}Ca+^{244}Pu\rightarrow^{288}114+4n$; and (c) $^{48}Ca+^{244}Pu\rightarrow^{289}114+3n$. For the spontaneous fission fragments, the values of the energies deposited in the front and side detectors are indicated. For all registered signals, the position coordinate is also given (Oganessian, Yeremin, Gulbekian, *et al.*, 1999; Oganessian *et al.*, 1999a, 1999b).

considerably limit the range of possible masses for the implanted nuclei, which is especially important in the cases in which the decay chains do not end in a region of known nuclei or in which the implanted evaporation residue already undergoes fission.

2. Experiments at the gas-filled separator GNS

The isotopes ^{265}Sg and ^{266}Sg were synthesized for the first time at the Dubna gas-filled separator GNS in the irradiation of ^{248}Cm with ^{22}Ne (Lazarev *et al.*, 1994). The experiment initiated a series of irradiations at the upgraded GNS, which culminated in the still ongoing investigation of element 114. The experiments were performed at Dubna in a collaboration between FLNR and LLNL, Livermore, California. In the $Z=106$ experiment, six α-fission event pairs were measured and assigned to ^{266}Sg, and four α-α correlations were assigned to ^{265}Sg. The α energies were 8.63 MeV and 8.71–8.91 MeV, respectively. These energies are rather low, and half-lives could be estimated to be in the range of 10 s. Due to missing implantation signals, an experimental half-life value could not be obtained in this first experiment. The observation of α decay of such low energy (and resulting long half-life) implied that ^{265}Sg and ^{266}Sg must have at least similarly long partial fission half-lives.

The result was not surprising after the shell effects at $N=162$ had been worked out theoretically in more detail. The measured α-decay data were in good agreement with the predictions by Ćwiok *et al.* (1983), Patyk and Sobiczewski (1991), and Smolanczuk and Sobiczewski (1995a, 1995b) and thus gave further evidence for the shell effect at $N=162$. The nonobservation of fission with short half-lives excluded the possibility of compact fission into symmetric fragments as discussed by Möller and Nix (1992). The data were later confirmed and extended by Türler *et al.* (1998) using the same reaction, but with an on-line gas chemistry apparatus (OLGA) for the separation of seaborgium and the study of its chemical properties (Schädel, Brüchle, Schausten, *et al.*, 1997; Schädel, Brüchle, Dressler, *et al.*, 1997). The experimental half-lives are 7.4 s (^{265}Sg) and 21 s (^{266}Sg). The experimental cross sections were evaluated to be 240 pb for the $5n$ channel and 25 pb for the $4n$ channel for a beam energy between 120 and 124 MeV.

The elements hassium and 110 were investigated in experiments using a ^{34}S beam and targets of ^{238}U and ^{244}Pu, respectively (Lazarev *et al.*, 1995, 1996). Three decay chains of the isotope ^{267}Hs were measured at a cross section of 2.5 pb. The decay data could be confirmed by the decay chain of ^{271}110 measured at SHIP (Hofmann, 1998). A few candidates for ^{273}110 were measured from the ^{244}Pu irradiation. The production cross section was about 0.4 pb ($5n$ channel).

One of the chains, which was considered as the best candidate to originate from the decay of ^{273}110, gave an α energy of 11.35 MeV at a resolution of ± 51 keV and a lifetime of 394 μs. The α decay of isotope ^{273}110 was also observed in the SHIP experiment, subsequent to the decay of ^{277}112 (see Fig. 4). The α energy was 11.08 MeV at an error bar of ± 20 keV, and the lifetime was 110 μs. Although the deviations are relatively large, a common origin cannot be excluded. The assignment to an isomeric state is another possibility. The decay of the granddaughter ^{269}Hs was not observed in the Dubna experiment. Therefore the time interval of 158 s between the decay of ^{273}110 and ^{265}Sg measured by Lazarev *et al.* (1995, 1996) includes the lifetime of ^{269}Hs. The corresponding averaged value from the respective decays in the two GSI chains is 29 s. However, the mean value including the Dubna data is 72 s, which is compatible with both results.

In November-December, 1998, an experiment aimed at synthesizing element 114 was performed at the GNS (Oganessian *et al.*, 1999a). A target of ^{244}Pu (0.4 mg/cm^2

thickness) was irradiated for a period of 34 days with a ^{48}Ca beam. The beam energy was 236 MeV at the target's center thickness, corresponding to the calculated maximum of the $3n$ evaporation channel. The excitation energy of the compound nucleus was estimated to range from 34 to 38.5 MeV. A total dose of 5.2×10^{18} projectiles was collected. One decay chain, shown in Fig. 12(c), was extracted from the data. The chain was claimed as a candidate for the decay of ^{289}114. The measured cross section was 1 pb.

The ^{48}Ca+^{244}Pu experiment was repeated in June – October, 1999. During a period of 3.5 months, a beam dose of 1.1×10^{19} ions was accumulated. Two more α-decay sequences, terminating in spontaneous fission, were observed (Oganessian *et al.*, 1999b). Both chains are displayed in Fig. 12(b). The two chains are identical within the statistical uncertainties and detector-energy resolution, but differ from the chain displayed in Fig. 12(c). The beam energy for the individual reaction was determined from the implantation energy and the knowledge of the momentarily irradiated target segment possessing an individual, but known, thickness. The estimate resulted in an excitation energy of (38 ± 2) MeV, which is a most probable value for a $4n$ evaporation channel. The two events were assigned to the decay of ^{288}114. The cross section was 0.5 pb.

The two newly measured chains are of high significance. The data reveal internal redundancy, and the lifetimes are short, making an origin from chance events unlikely. The assignment to the $4n$ channel is likely, but the objections that we made at the end of the previous subsection also hold true here. A comparison of the measured data with theoretical predictions will be given in Sec. V.

E. The reaction ^{86}Kr+^{208}Pb→^{294}118* studied at the Berkeley gas-filled separator and at the GSI SHIP

After the shutdown of the SuperHILAC linear accelerator in Berkeley, ideas were discussed for building a new efficient separator for fusion-reaction products at the 88-Inch Cyclotron. The first design of a Large-Angle Separator System (LASSY) was rejected. This was a gas-filled separator utilizing superconducting magnet technology. The large costs and the long time scale necessary for LASSY construction led to a parallel effort to design a separator based on normal-conducting magnet technology, which could be built much more economically and on a much faster time scale (Gregorich *et al.*, 1996).

The final version of the BGS (Berkeley Gas-filled Separator) was described by Ninov *et al.* (1998). It consists of three magnets, a vertically focusing quadrupole magnet followed by a strong horizontally focusing gradient-dipole magnet and a flat-field dipole magnet. The maximum rigidity of the separator is 2.5 Tm, and the total bending angle is 70°. This is an unusually large bending angle, but it provides high background suppression for reactions with lead targets up to the heaviest beams (krypton) that can be delivered by the cyclotron.

The BGS became ready for the first experiments by 1998. In the autumn of the same year, Smolanczuk (1999a) was working on a theoretical study, "Production mechanism of superheavy nuclei in cold-fusion reactions." Using a relatively simple fusion model, he reproduced the measured formation cross sections of deformed heavy nuclei synthesized in cold-fusion reactions from No, $\sigma=260$ nb, to $Z=112$, $\sigma=1$ pb. The same model, applied for the calculation of cross sections for the synthesis of spherical superheavy nuclei, resulted in the unusually high value of 670 pb for the reaction ^{86}Kr+^{208}Pb→^{293}118+1n.

In order to prove the validity of the theoretical prediction for the synthesis of element 118, Ninov *et al.* (1999) performed an irradiation for five days from April 8 to April 12, 1999. The fact that the beam of noble-gas krypton could easily be produced from an electron cyclotron resonance ion source available at the cyclotron was particularly helpful.

The energy of the ^{86}Kr beam was 459 MeV. The projectiles had to pass through an entrance window into the gas-filled chamber of the separator of 0.1 mg/cm^2 carbon and the target backing of 40 μg/cm^2 carbon before they entered the ^{208}Pb-target layer, which was 300–450 μg/cm^2 thick. The targets were mounted on a wheel of 155-mm radius up to the center of the targets that was rotated at 400 rpm. The beam energy in the middle of the target thickness corresponded to a calculated excitation energy of the compound nucleus of about 13 MeV. The separator efficiency for this reaction was estimated to be 75%. The detector system was similar to the one at SHIP: a position-sensitive silicon strip detector was used as a central detector, but no detector was mounted in the back hemisphere for the measurement of escaping α particles. In front of the silicon detector, a parallel-plate avalanche counter was used instead of secondary electron foil detectors. Behind the silicon detector, a second silicon strip "punchthrough" detector was installed to reject particles passing through the primary detector. The dead time of the data acquisition system was 120 μs.

Two event chains, consisting of an implanted evaporation residue and of subsequently emitted α particles, were observed at a beam dose of 0.7×10^{18} ions. The resulting cross section was 4.8 pb. An analysis of the statistical error bars for the two events according to Schmidt *et al.* (1984) gives values of $^{+6.0}_{-3.1}$ pb.

The experiment was repeated in Berkeley from April 30 to May 5, 1999. During the six days of irradiation a beam dose of 1.6×10^{18} ions was collected, and one more chain was observed. The cross section resulting from the second irradiation is 1.1 pb, with a purely statistical error of $^{+2.5}_{-0.9}$ pb. The cross section from the two parts of the experiment as given by Ninov *et al.* is $(2.2^{+2.6}_{-0.8})$ pb. The three chains observed are shown in Fig. 13 along with their assignment to the superheavy nucleus ^{293}118.

The experimental data suffer slightly from the fact that no detectors were mounted in the back hemisphere, and therefore 7 of the total of 19 signals did not contain the full α energy. However, the signals were high

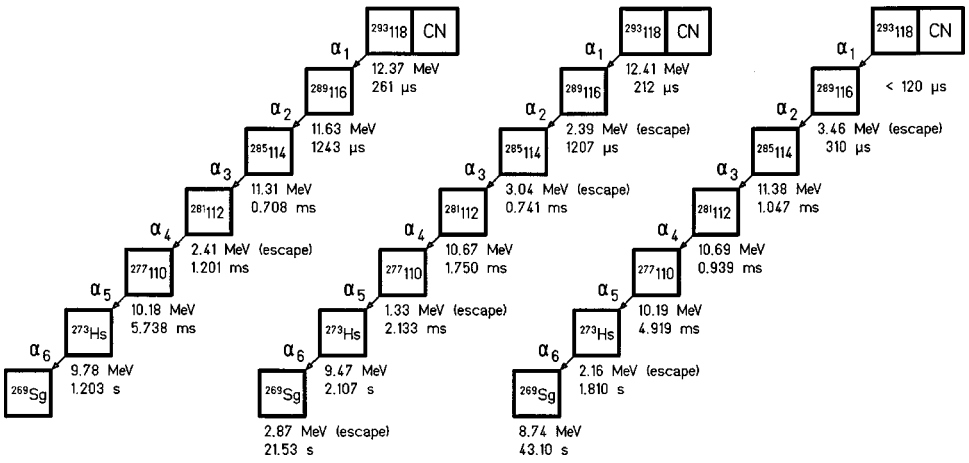

FIG. 13. Decay chains and assignment obtained in experiments at Berkeley using the reaction $^{86}Kr+^{208}Pb\rightarrow^{294}118^*$. The "escape" α particles are emitted towards the front of the detector and deposit only a fraction of their energy in the detector. From Ninov *et al.*, 1999.

enough to provide time information and allow for a reasonable assignment to α particles. The first α decay of the third chain was very likely lost because of a relatively long dead time. The α energies of the decays assigned to $^{293}118$, $^{285}114$, $^{281}112$, and $^{277}110$ reveal some internal redundancy. They each appear twice within the limits set by the detector resolution. The lifetimes up to the fifth α decay are short, on the order of one millisecond, which makes an origin by chance coincidences extremely unlikely. An origin due to electric disturbances is excluded by the authors (Ninov *et al.*, private communication). The assignment of the events to the decay of $^{293}118$ is most likely at the low excitation energy of the compound nucleus.

In order to confirm the data obtained in Berkeley, we investigated the same reaction at SHIP in the summer of 1999. For the purpose of controlling our setup, we first repeated the known reaction $^{58}Fe+^{208}Pb\rightarrow^{265}Hs+1n$. At a beam energy of 283.8 MeV, which is at the maximum of the excitation function, we measured a total of 16 events during two days. The resulting cross section was (98 ± 25) pb, in agreement with the previously known maximum value (Hofmann *et al.*, 1995a). The test demonstrated that the UNILAC energy and the electromagnetic field settings of SHIP are reproducible and that the analysis program is working properly.

In a second step, we measured excitation functions of the $2n$, $3n$, and $4n$ evaporation channels of the reaction $^{86}Kr+^{120}Sn\rightarrow^{206}Rn^*$ for comparison with the data obtained in Berkeley for the same reaction. The aim of this experiment was to adjust the beam energy of the two accelerators, which is important in the case of narrow excitation functions. The results obtained showed that the location of the excitation functions from the two experiments was accurate only within ±2.0 MeV in excitation energy. That result points to a possible deviation of the beam energies between the 88-in cyclotron and the UNILAC of ±3.4 MeV, and to an uncertainty of ±2.4 MeV in excitation energy for the reaction $^{86}Kr+^{208}Pb\rightarrow^{294}118^*$. This uncertainty is unsatisfactory in view of the narrow excitation functions expected for the synthesis of heavy elements in cold-fusion reactions. For example, an excitation energy value of 4.8 MeV was measured for the full width at half maximum (FWHM) for the reaction $^{58}Fe+^{208}Pb\rightarrow^{265}Hs+1n$. The literature value given for the accuracy of the beam energy at the 88-Inch Cyclotron is ΔE (FWHM)=2.3 MeV for a ^{86}Kr beam of 459 MeV (Ninov *et al.*, 1999), and at the UNILAC, ΔE (FWHM)=1.7 MeV for the absolute energy and ΔE (FWHM)=0.5 MeV for the relative energies (Hofmann *et al.*, 1995a). These values are important for extracting the widths of excitation functions.

Besides the value of the beam energy, the width and the long-term stability of the energy are also important parameters of the beam quality. These parameters strongly depend on the settings of the accelerator, and they usually vary within a certain range. For the UNILAC, we estimated that the width of this range is smaller than 2 MeV (FWHM).

The first part of the main experiment started at SHIP on June 7, 1999. We chose a beam energy of 453.9 MeV, resulting in the same excitation energy of the compound nucleus at the target's center thickness as in the Berkeley experiment. During nine days of irradiation, we collected a projectile dose of 1.0×10^{18}. The cross-section limit obtained was 2.8 pb. We continued the irradiation using the same beam energy on July 26. Over a period of 15.5 days, we reached a projectile dose of 1.9×10^{18}. In the second run, we again did not observe any chain similar to those observed at Berkeley. The cross-section limit resulting from both parts of the experiment is 1.0 pb at an excitation energy of 13.3 MeV. Our cross-section values are based on a total efficiency of 50%.

In addition, we did a relatively short irradiation of three days using a slightly higher beam energy of 456.7 MeV, which resulted in an excitation energy higher by 2.3 MeV. The reason for this additional irradiation was the predicted steep decrease of the cross section (Smolanczuk, 1999b) at the low-energy side of the excitation function. Therefore a beam energy slightly too low could result in a significant loss of production yield, as could already have been the case in the Berkeley experiment. At the higher energy, as well, we did not observe any long α-decay chain. From a dose of 0.4×10^{18} projectiles, we deduced a cross-section limit of 6.8 pb.

In our experiment, we could not confirm the Berkeley data on the synthesis of $^{293}118$. However, our negative

result does not disprove those data. Several possible reasons could plausibly explain the difference:

(1) A probability analysis based solely on statistical distributions still gives a probability of 17% that, in two experiments at approximately the same beam dose, three events could be observed in one case and zero in the other.

(2) The beam energy from the 88-in cyclotron and from the UNILAC may differ by more than 2 MeV, which could result in a significantly lower cross section in our experiment.

(3) We calculated a mean ionic charge state of 32^+ for the $^{293}118$ residue escaping from the target and the charge equilibration foil using the empirical formula of Nikolaev and Dmitriev (1968). If the real value differed by more than 10%, our transmission through SHIP up to the focal plane would be reduced by more than 50%.

(4) Isomeric states have been observed in many odd and odd-odd nuclei in the region of heavy elements up to $Z=112$. The predicted level structure of $^{293}118$ (Ćwiok and Nazarewicz, 1999) reveals low and high spin levels close to the ground state, which could result in the formation of isomeric states. A decay of the isomer after passing through the charge equilibration foil could significantly change the ionic charge state of $^{293}118$. At a half-life of the isomer between 20 ns and 1 μs, more than 50% of the residues could be lost due to unexpected ionic charge states. The lower half-life value is determined by the distance of 16 cm of the charge equilibration foil downstream from the target, and the upper value by the 11-m length of SHIP. The problem of charge changing decays of isomeric states is absent or at least less significant at gas-filled separators because a mean charge state is reached within short distances in the gas. However, the mean value of the charge state in pure helium gas is only about 10^+. At such low charge states, a simple trend, as a function of the element number and the velocity, is modulated by shell effects of the electrons and by impurities in the helium gas. Deviations of the ionic charge state are of great consequence at high deflection angles of the separator, as in the case of the 70° deflection angle of the Berkeley gas-filled separator.

Further attempts to confirm the Berkeley data will be made by repeating the experiment at the BGS itself. The experiment is planned for early in the year 2000 after an upgrade of the detector and the data acquisition system. Measurements at several different beam energies are also planned. It seems possible that the cross section may even be higher than 2.2 pb at slightly higher or lower beam energies. This would be a very positive result for the further investigation of nuclei in the superheavy elements region.

V. GROUND-STATE PROPERTIES OF SUPERHEAVY ELEMENTS

A. Ground-state binding energy and deformation

Shell-model calculations based on the Strutinsky approach are most successful in reproducing the measured nuclear binding energies. Experimental values are obtained by correlation of the α-decay data with decay-chain nuclei of known masses. Figure 14 shows a plot of deviations of various calculated data from the experimental values. Significant deviations of some of the calculated values of up to 3 MeV arise for nuclei for which bigger shell gaps determine the binding energy, here at $Z=110$, $N=162$. However, for odd nuclei, an uncertainty in the experimental data arises, because α transitions either to excited levels or from isomeric states cannot be excluded.

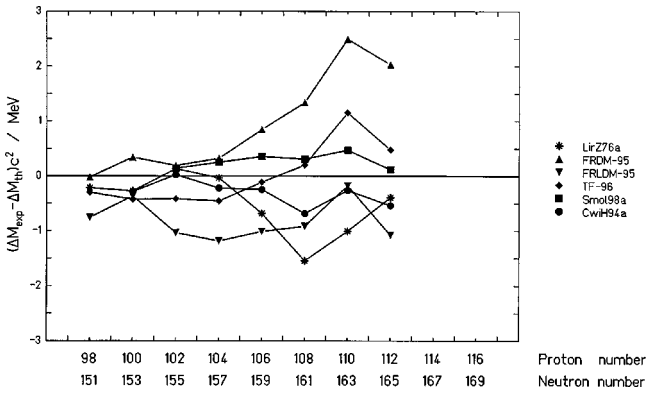

FIG. 14. Comparison of calculated mass excesses with the experimental data for nuclei of the α-decay chain of $^{277}112$. The predicted values are from Liran and Zeldes (1976; LirZ76a), Möller *et al.* (1995a, 1995b; FRDM-95, FRLDM-95), Myers and Świątecki (1996; TF-96), Smolanczuk (1997, 1998), and Ćwiok *et al.* (1994).

Möller, Nix, and Kratz (1997) have calculated proton and neutron single-particle level diagrams for spherical and deformed nuclei. The diagrams are useful in providing the spin and parity of low-lying states of odd-even nuclei and in identifying gaps in the level spectra that may be associated with exceptionally stable proton-neutron combinations. As an example, the results for the $^{272}110$ nucleus are given in Fig. 15.

One particularly interesting fact in the region of heavy elements is that deformed shell gaps at proton numbers $Z=108-110$ and neutron number $N=162$ emerge only for relatively large negative values of the hexadecapole deformation parameter β_4. These gaps give rise to unusual stability, which in turn yields long enough half-lives, making the observation of elements 107 to 112 possible. Similarly, the gaps in the level spectra at proton number $Z=100$ and neutron number $N=152$ (see Figs. 47 and 48 in Möller, Nix, and Kratz, 1997) lend an extra degree of stability to the isotones near ^{252}Fm. This is indicated by the partial fission half-lives of those isotopes (see Fig. 7 in the paper by Patyk *et al.*, 1989). The good agreement of the experimental value $\beta_2=0.27\pm0.02$ (Reiter *et al.*, 1999) of ^{254}No with the calculation (Patyk and Sobiczewski, 1991; Möller *et al.*, 1995a, 1995b; Muntian *et al.*, 1999) strengthens the predictive power of the theory. The fact that this extra stability connected with $N=152$ extends up to and includes seaborgium was discussed in Sec. III.B, Fig. 6. At $N=152$, however, the hexadecapole deformation param-

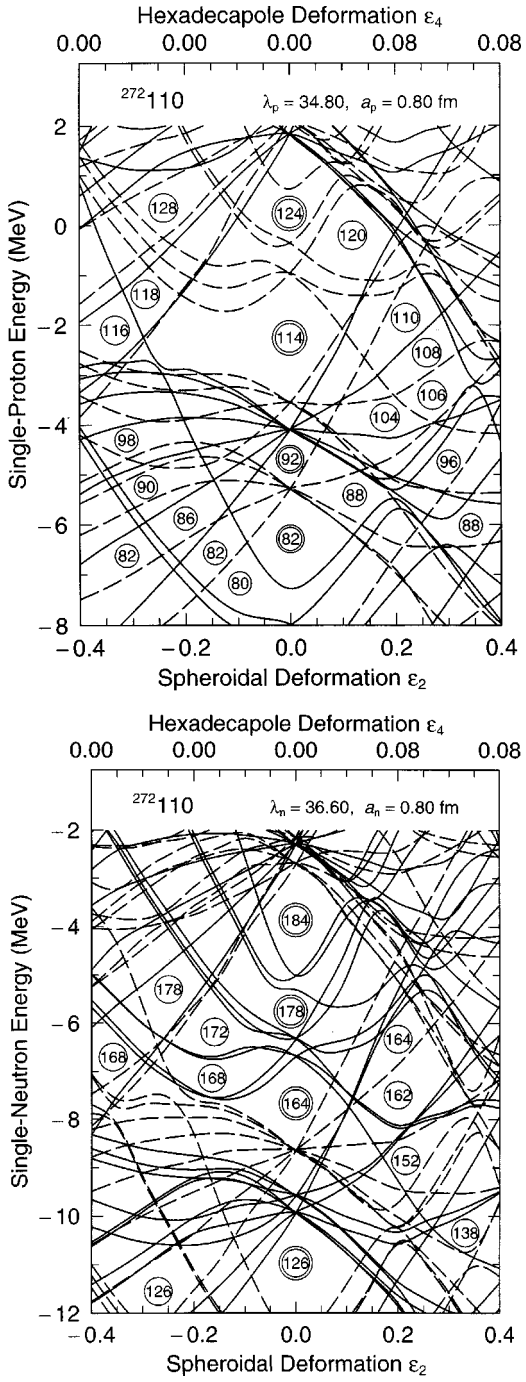

FIG. 15. Calculated single-particle level diagrams for nuclei in the vicinity of $^{272}110_{162}$, which is calculated as being deformed in its ground state: (a) proton; (b) neutron. From Möller, Nix, and Kratz, 1997.

eters approach zero (Möller, Nix, and Kratz, 1997). For smaller proton and neutron numbers, these parameters decrease to large negative values, reaching a minimum near $N=140$ and $Z=90$ (see Fig. 12 in Möller and Nix, 1994).

The feasibility of extracting semiquantitative values for the hexadecapole moment (including the sign) has been presented by Zamfir *et al.* (1995). They used the fact that a number of spectroscopic observables lie along smooth curves when plotted against the product of valence proton and neutron numbers, N_pN_n. Zamfir *et al.* studied the behavior of $B(E2;2_1^+\rightarrow 0_1^+)$ along with a defined value $B(E2;2_1^+\rightarrow 0_1^+)_Q$, which is a correction for the effect of the hexadecapole moment β_4 on the $B(E2)$ value, as a function of N_pN_n. Application of this method to the region of superheavy nuclei led them to conclude that $Z=126$ was the dominant shell closure affecting both nuclear structure and its evolution in the transactinide region.

In a series of papers (Ahmad *et al.*, 1977, 1990; Chasman *et al.*, 1977; Chasman and Ahmad, 1997), the level spacings and level orderings of odd nuclei in the $A\approx 250$ mass region were investigated in an effort to fit the parameters of a Woods-Saxon potential and extrapolate the values into the *vis-à-vis* region of superheavy nuclei. The position of the $1/2^-[521]$ Nilsson proton orbital is crucial in this procedure. This orbital originates in the $\pi f_{5/2}$ subshell, a subshell that is filled beyond proton number 114. Therefore the energy of the $1/2^-[521]$ state is significantly influenced by the $f_{7/2}$–$f_{5/2}$ spin-orbit splitting, which determines the energy gap at $Z=114$.

Recently, several attempts were made to understand the shell structure properties of SHE's based on the self-consistent and relativistic mean-field theory (Ćwiok *et al.*, 1996; Lalazissis *et al.*, 1996; Rutz *et al.*, 1997; Kruppa *et al.*, 2000). Ćwiok *et al.* compared the results of the macroscopic-microscopic method with a Hartree-Fock calculation. There are several factors influencing the calculations, thus making them uncertain especially in the region of SHE's. The most important one is the large mass and the large electric charge of a superheavy nucleus. With increasing A, the single-particle spectrum becomes more compressed and the binding energy increases due to increased range (radius) of the average potential. Moreover, the energy of orbitals with $l=\mathcal{N}$, $j=l-1/2$, such as $1h_{9/2}$, $1i_{11/2}$, $1j_{13/2}$, are lowered considerably due to a weakened spin-orbit splitting at large values of mass A (see Sobiczewski *et al.*, 1966; Meldner, 1967; Figs. 2–30 in the book by Bohr and Mottelson, 1969; Nilsson, 1978; Mairle, 1995). Further influence on the shell structure arises from the nuclear surface diffuseness as reinvestigated recently by Myers and Świątecki (1998). Using the Thomas-Fermi model, they treated the diffuseness as a free parameter in a macroscopic-microscopic calculation. They found that an increase of the diffuseness parameter of a heavy nucleus by 10% costs about 4-MeV binding energy in the macroscopic part, but the total gain in shell-effect energy is 12 MeV at $Z=126$ and $N=184$, thus shifting the magic proton number from 114 to 126.

Actually, the location of the three low-spin proton subshells $2f_{5/2}$, $3p_{3/2}$, and $3p_{1/2}$, which are filled between $Z=114$ and $Z=126$, is the factor that determines the stability landscape of SHE's. Qualitatively, we may expect the minimum of the negative shell-correction energies to be wide and not as deep if the low-spin proton orbits are equally distributed in energy between $Z=114$ and $Z=126$. The fission barriers will then also be

flat and narrow, their height and width being mainly determined by the shell-correction energy. As a result, the fission half-lives will be relatively short. On the other hand, if there is a wide energy gap beyond one of the proton numbers 114, 120, or 126, then the shell-correction energies will be pronounced for that element. In combination with the neutron shell effect at $N=184$, a sharp and deep minimum will be formed, similar to that of the doubly magic ^{208}Pb, resulting in a high fission barrier and relatively long fission half-life. The α half-lives will also be more strongly modulated by great shell effects, resulting in long α half-lives below and short half-lives above the magic number.

In the case of a deep minimum of the shell-correction energy, there could even be a correlation between stability and production cross section that could result in an enhanced cross section even for the highest proton number. The observed reduction of fusion probability for the elements up to $Z=112$, due to the separation of projectile and target nucleus by the increasing Coulomb forces, may be compensated for by strong attractive shell effects. The measured cross sections, in the range of 0.5–5 pb for the synthesis of elements 114 and 118, seem to indicate such an influence. Because of the remaining uncertainties of the model calculations, further experimental investigations are of great importance.

B. Decay properties of superheavy elements

In order to estimate the decay properties of nuclei that may eventually become possible to produce, some extrapolation into the region of SHE's is necessary. The predictions set forth by the macroscopic-microscopic models are extremely useful for extrapolation into this region. Figure 16 presents the results of calculations by Smolanczuk and Sobiczewski (1995a, 1995b), Smolanczuk (1997, 1998), and Möller *et al.* (1995a, 1995b).

The shell-correction energy plays a major role in the determination of the fission barrier. Therefore the contour maps of the shell effects and the fission half-life are similar in appearance [Figs. 16(a) and (b)]. Notwithstanding the shared shell-correction energy minimum of -7 MeV, the fission half-life only reaches a value of 1000 s for the nuclei at $Z=108$, $N=162$. This is a direct result of the deformed ground state and hence more narrow fission barrier. The fission barrier is wider for the spherical nuclei, and the fission half-lives increase up to 10^{12} s$=32\,000\,y$.

The dominating partial half-life is shown in Fig. 17(a) for even-even nuclei. The two regions of deformed heavy nuclei near $N=162$ and spherical SHE's merge and form a region of α emitters surrounded by fissioning nuclei. The longest half-lives are 1000 s for deformed heavy nuclei and 30 y for spherical SHE's. It is interesting to note that the longest half-lives are not reached for the doubly magic nucleus $^{298}_{184}$114, but for $Z=110$ and $N=182$. This is a result of the continuously increasing Q_α values with increasing element number. Therefore α decay becomes the dominant decay mode beyond element

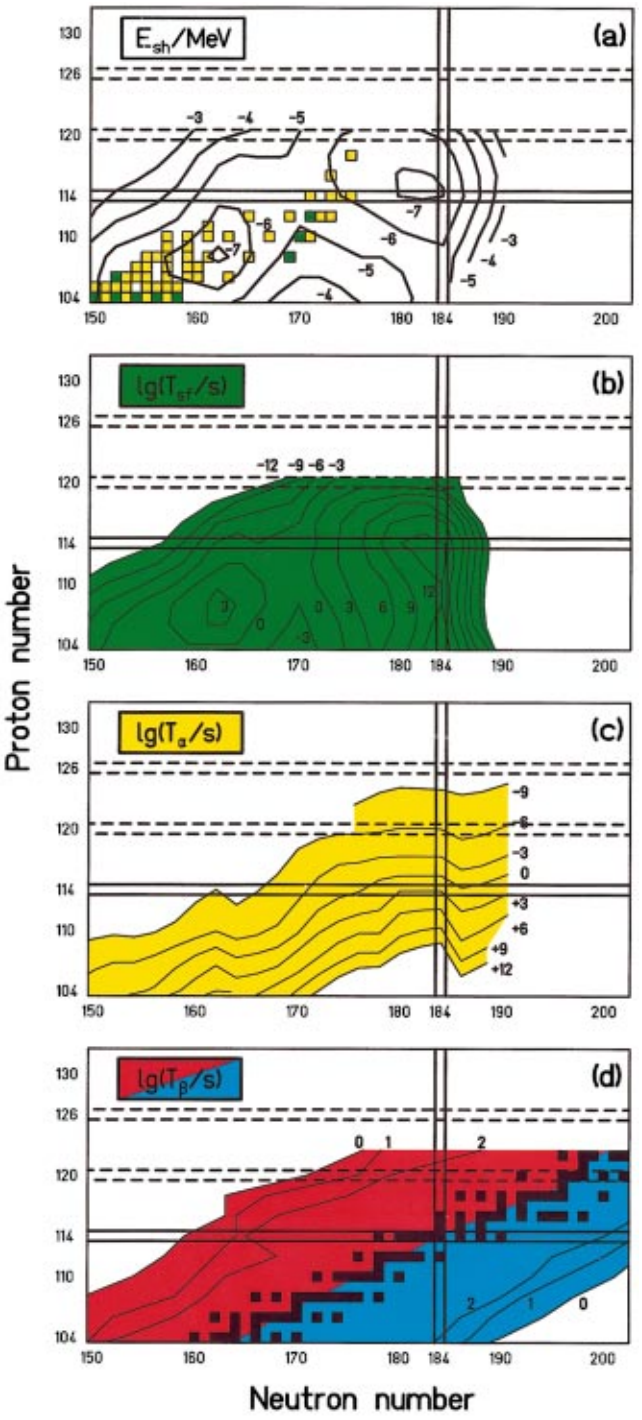

FIG. 16. The decay properties of heavy and superheavy nuclei according to macroscopic-microscopic calculations: (a) ground-state shell-correction energy; (b) partial fission half-life of even-even nuclei; (c) unhindered α-decay half-life; (d) β^+ and β^- half-life. The β-stable nuclei are marked by filled squares. The predicted values in (a), (b), and (c) are from Smolanczuk and Sobiczewski (1995a, 1995b) and Smolanczuk (1997, 1998), and in (d) from Möller *et al.* (1995a, 1995b) [Color].

110 with continuously decreasing half-life. The half-lives of nuclei at $N=184$ and $Z<110$ are reduced from β^- decay.

The three-member decay chain of ^{288}114, the heaviest even-even nucleus, observed in the recent experiment in

Dubna (Oganessian *et al.*, 1999b), is also drawn in Fig. 17(a). The arrows follow approximately the 1-s contour line down to $^{280}110$, which is, in agreement with the experiment, predicted to be a spontaneously fissioning nucleus. The experimental half-lives are 2–10–7 s, respectively, which is longer than the calculated values by a factor of 10 on average. However, this deviation is well within the accuracy limits of the calculation. For example, a change in the α energy of $^{288}114$ by 350 keV only changes the half-life by a factor of 10.

For detection purposes, the neutron-deficient even-even nuclei that are reached in both cold and hot fusion reactions [Fig. 17(c)] are ideal cases. The isotopes between element 108 and 120 are predicted to decay by α emission with half-lives in the range 1 μs–1 s. The decay chains will end by fissioning nuclei with $T_{1/2} \approx 1000$ s in the region near $Z=106$ and $N=162$. In contrast to this, nuclei with half-lives of several hours or longer produced at low cross sections ($\leqslant 10$ nb) are difficult to measure using the current experimental techniques.

In the case of odd nuclei [Fig. 17(b)], the α and fission half-lives calculated by Smolanczuk and Sobiczewski (1995a, 1995b) were multiplied by a factor of 10 and 1000, respectively, thus making provisions for the odd-particle hindrance factors. However, we have to keep in mind that the fission hindrance factors have a wide distribution from 10^1 to 10^5, which is mainly a result of the specific levels occupied by the odd nucleon. For odd-odd nuclei (not shown here), the fission hindrance factors from both the odd proton and the odd neutron are multiplied. The β half-lives given by Möller, Nix and Kratz (1997) were divided by 10, because first-forbidden transitions were not taken into account in these calculations (see Möller, Nix, and Kratz 1997a and discussion therein). For the odd nuclei, the island character of the α emitters disappeared and α decay could propagate down to rutherfordium and beyond. In the allegorical representation where the stability of SHE's is seen as an island in a sea of instability, the even-even nuclei portray the situation during a flood, the odd nuclei during an ebb, when the island is connected to the mainland.

The decay chains of the recently measured even-odd nuclei are also drawn in the figure: $^{277}112$, GSI-Darmstadt, $^{287}114$ and $^{289}114$, JINR-Dubna, and $^{293}118$, LBNL-Berkeley. Here again, the measured data are predominantly well duplicated in the calculations. The assignment of the three chains observed in Berkeley finds particularly strong support in the excellent agreement with the predicted half-lives (or vice versa). The greatest disagreement seems to exist in the case of $^{283}112$, which is predicted to α decay with a half-life of about 1 s, whereas fission with a half-life of 180 s was measured at Dubna. However, an explanation for this deviation may be found in different hindrance factors for α decay and fission or in the occurrence of isomeric states.

Figure 17(c) shows the known nuclei at present and compound nuclei that could be formed by reactions with ^{208}Pb or ^{248}Cm targets and stable projectile isotopes, plotted on the contour map of shell-correction energies. The region of relatively long-lived deformed heavy elements is well covered by reactions with ^{248}Cm targets or the α-decay products of reactions with ^{208}Pb targets. This is not the case for the central region of spherical SHE's. A close approach is possible using the reactions $^{82}\mathrm{Se}+^{208}\mathrm{Pb}\rightarrow^{290}116^*$, $^{86}\mathrm{Kr}+^{208}\mathrm{Pb}\rightarrow^{294}118^*$, $^{48}\mathrm{Ca}+^{248}\mathrm{Cm}\rightarrow^{296}116^*$, and $^{50}\mathrm{Ti}+^{248}\mathrm{Cm}\rightarrow^{298}118^*$. An even closer approach may become feasible in the future with the use of neutron-rich radioactive beams.

In the case of strong shell-correction energies at $Z=126$ and $N=184$, this region of SHE's would be easily accessible with stable projectiles in both cold and hot fusion reactions with targets of lead or isotopes of the actinide elements. However, short α half-lives below 1 μs may prevent direct observation.

VI. SYNTHESIS OF SUPERHEAVY ELEMENTS

A. Excitation functions

A summary of recently measured even-element excitation functions is shown in Fig. 18. On the left side, the cross sections are plotted as a function of the dissipated energy E^*, calculated from the center-of-mass beam energies in the middle of the target thickness and the Q values. The Q values were determined from the experimental masses of projectile and target evaluated by Audi and Wapstra (1993) and the mass for the compound nucleus predicted by Myers and Świątecki (1996). The arrows mark the energy E^*, which is obtained from the beam energy necessary to reach the contact configuration according to the fusion model of Bass (1974). On the right side, the neutron binding energies according to Myers and Świątecki are subtracted. The resulting free reaction energy is a sum of the kinetic energy of the emitted neutrons and the energy of emitted γ rays. The continuous curves are Gaussian fits through the data points, and the dashed curve ($Z=112$) is extrapolated.

The cross-section trend of the $1n$ evaporation channel is plotted in Fig. 19. Extrapolation of the curve into the region of heavier elements results in a cross section of about 1 fb for the synthesis of element 116. Higher cross sections may be expected if the trend of the data, namely increasing cross section with increasing isospin, continues. This effect was proved in the production of element 110 using the projectiles ^{62}Ni and ^{64}Ni. The systematics was not confirmed in the synthesis of elements 112 and 113 using the $T_z=5$ projectile ^{70}Zn. In these two cases, however, a single, relatively low beam energy was used. It seems possible that the cross section may increase at slightly higher beam energies. An experimental proof is in preparation at SHIP.

The cross-section trend is completely changed by the Berkeley result on the synthesis of element 118 (Ninov *et al.*, 1999). Even with an optimistic extrapolation, taking into account a cross-section increase by a factor of 3.5 with a projectile whose isospin is higher by one unit for each subsequent even element, a value of 0.1 pb only could be obtained for the reaction $^{86}\mathrm{Kr}+^{208}\mathrm{Pb}\rightarrow^{293}118+1n$. A possible explanation may reside in strong shell effects at $N\approx 175$ and $Z=114-118$, combined with a

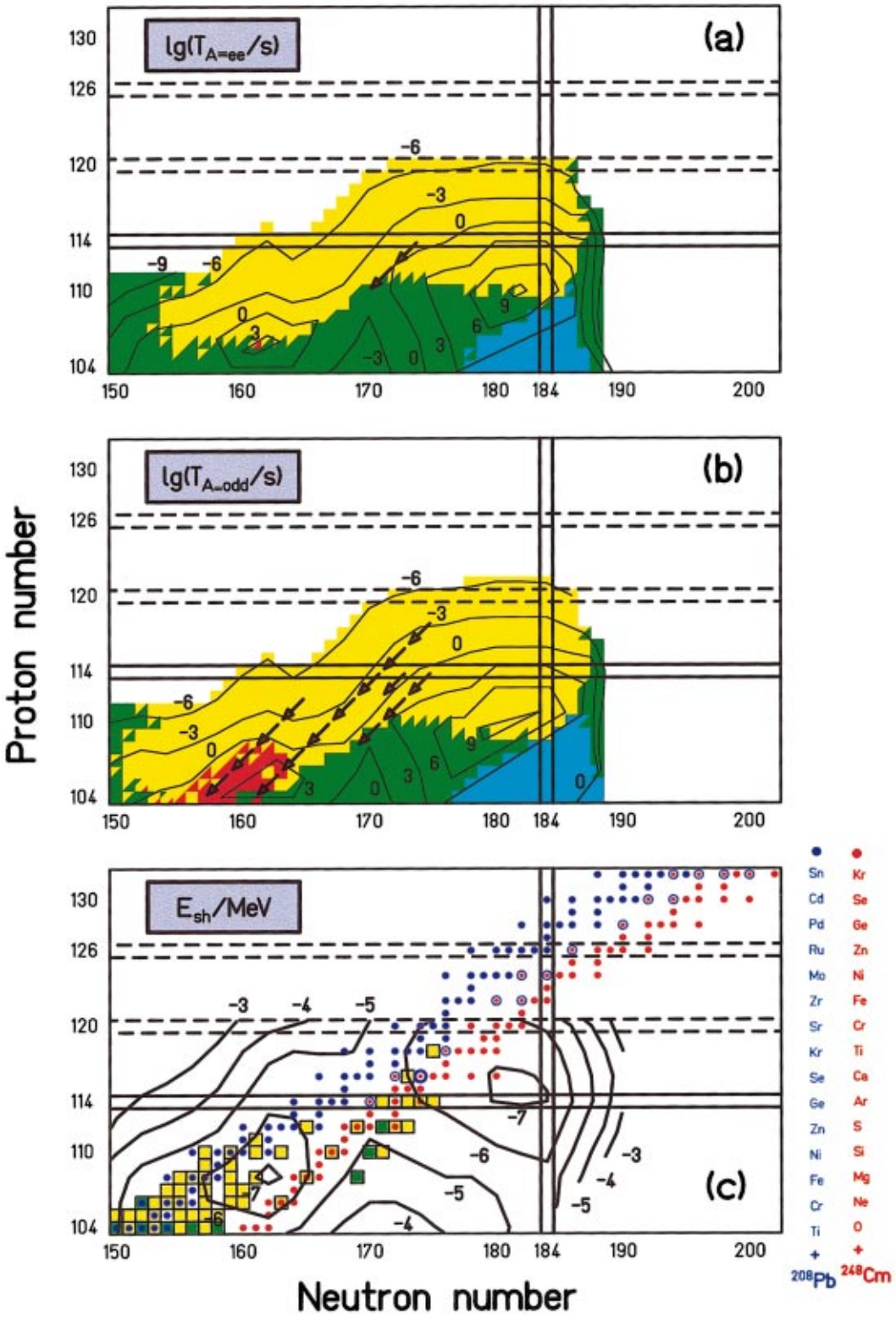

FIG. 17. Dominating partial α, β, or fission half-life: (a) for even-even nuclei; (b) for odd-A nuclei. The bold lines separate regions of dominant α decay, β decay, and spontaneous fission. Diagram (c) shows the ground-state shell-correction energy and compound nuclei, which can be reached in reactions with targets of ^{208}Pb or ^{248}Cm and stable projectile isotopes. The nuclei known at present are marked by filled squares. The sequence of arrows in (a) indicates the decay chain of ^{288}114 (Dubna) and the arrows in (b) those of ^{277}112 (Darmstadt), ^{287}114, ^{289}114 (Dubna), and ^{293}118 (Berkeley; see text) [Color].

transition from deformed to spherical nuclei. Both effects lower the fission probability of the compound nucleus, not only in the ground state, but also at low excitation energies. This is the main reason for the unusually high cross section of 670 pb calculated by Smolanczuk (1999a).

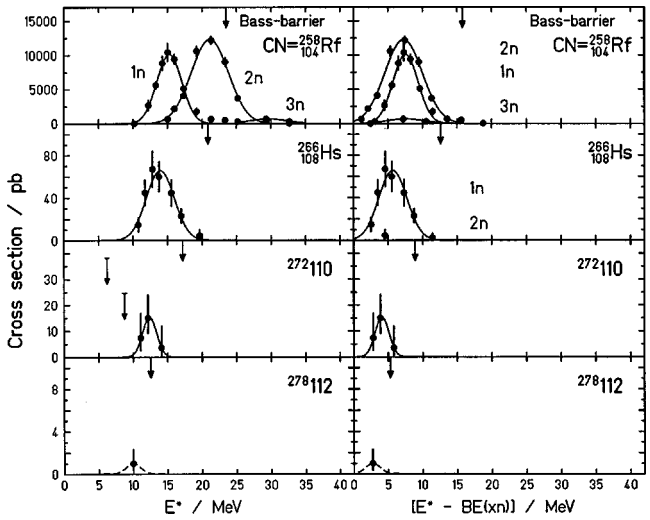

FIG. 18. Measured even-element excitation functions.

In all cases where excitation functions are known, the cross-section maxima on the right in Fig. 18 are approximately centered between zero and the energy needed to reach the contact configuration according to the Bass model. This empirical result seems to present a sound method for determining the position of the cross-section maxima in cold-fusion reactions.

A comparison of excitation energies at the barrier for cold and hot fusion reactions over a wide range of SHE's is shown in Fig. 20. A remarkable transition is observed from a region of high excitation energies (>40 MeV), for reactions with a ^{238}U target resulting in elements up to $Z \approx 114$, into a region of low excitation energies, down to 6 MeV for element 126. This reflects a change from hot fusion to cold fusion with regard to the excitation energy. However, the excitation energy is probably not the most important quality parameter for distinguishing between the two types of reaction. Another, possibly more important, difference could reside in the fact that, as a target, ^{208}Pb is a spherical closed-shell nucleus with empty shells above the shell closures, whereas ^{238}U is well deformed and midshell.

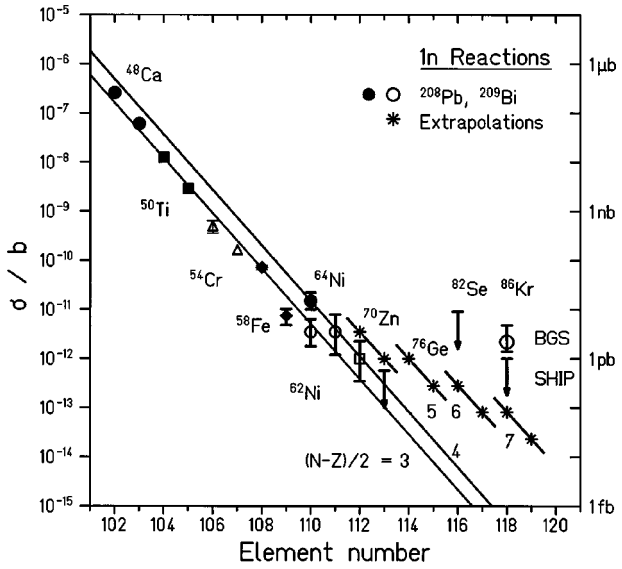

FIG. 19. Plot of cross-section data and extrapolated values for cold-fusion reactions ($1n$-evaporation channel). The line for isospin three is fitted to the data, and, for isospin four, shifted to cross the two data points ($Z=110$ and 111) obtained with a ^{64}Ni beam. The short lines are extrapolations (see text). The arrows mark the cross-section limits obtained at SHIP for elements $Z=116$ and 118. The data point labeled with BGS for $Z=118$ is from Ninov *et al.* (1999). Full symbols represent cross-section maxima obtained from excitation functions; in the case of open symbols, excitation functions are not yet known.

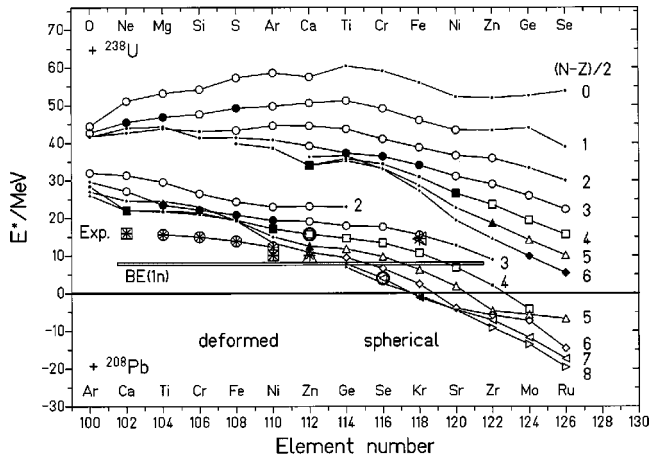

FIG. 20. Diagrams of excitation energies at the interaction barrier according to the model of Bass (1974). The upper cluster shows the trend for hot-fusion reactions with a ^{238}U target and projectiles between O and Se, and the lower cluster for cold-fusion reactions with a ^{208}Pb target and projectiles from Ar to Ru. The large symbols mark stable projectile isotopes, and the small symbols radioactive isotopes. The filled symbols of $T_z=4$, 5, and 6 nuclei in the upper part are enhanced because they impressively mark the transition from hot to cold fusion with increasing element number using actinide targets. The other filled symbols up to element 112 mark reactions investigated at SHIP by cold fusion or at Dubna by hot fusion. The star symbols mark the excitation energies, at which the maximum cross section was observed in cold-fusion reactions. The data point obtained at Berkeley from the reaction ^{86}Kr+^{208}Pb is also shown. The $1n$-binding energies are in a range from 7.5 to 8.2 MeV for the investigated cold-fusion compound nuclei and are marked by the horizontal bar.

Following the rule of maximum cross sections of cold-fusion reactions worked out by means of Fig. 18, the curves in Fig. 20 allow for the extrapolation of the trend beyond element 112. There is only a very narrow window of excitation energy left for the production of element 114 with a ^{76}Ge beam and $1n$ emission.

For element 116, the reactions with ^{82}Se and ^{80}Se already give rise to excitation energies at the barrier that are smaller than the $1n$ binding energy. In this case, the free energy can only be removed by γ rays. This so-called "radiative capture" channel was observed in the SHIP experiments for heavy ions in the reaction ^{90}Zr(^{90}Zr, γ's) ^{180}Hg (Keller *et al.*, 1983). It is not yet

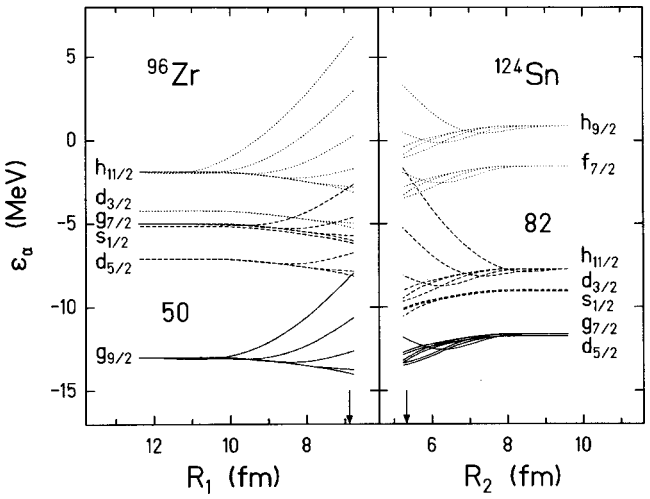

FIG. 21. Diabatic neutron levels as a function of the distances R_1 and R_2 of the potential centers from the center of mass for ^{96}Zr+^{124}Sn: solid lines, levels that are initially fully occupied; dashed lines, levels that are partially occupied; dotted lines, levels that are initially empty. From Berdichevsky *et al.*, 1989.

known in the region of SHE's where fission is a strong competition in the deexcitation of the compound nucleus.

Alternatively, the $1n$ channel may be investigated with neutron-deficient projectiles resulting in excitation energies greater than the $1n$ binding energy. This choice may become important if the reaction does not allow for an increase of the kinetic energy beyond the value determined by the contact configuration when the reaction partners come to rest in the center-of-mass system. The reason for an upper limit of the kinetic energy could be diabatic shifts of single-particle levels at higher kinetic energies at the very beginning of the reaction, which cause a repulsive force on the collective motion of the reaction partners to each other. This process was theoretically investigated by Nörenberg (1983).

The effect exists independently from the fissility of the reacting system. However, it is strongly determined by nuclear structure. An example is shown in Fig. 21. Diabatic level shifts demand extra energy for the fusion of medium-heavy nuclei and lead to an increased separation probability in the case of the heaviest systems because the surface tension is already compensated for by Coulomb forces. For light nuclei, the contracting surface tension is predominant, and the formation of a compound nucleus is overwhelming.

Prompted by the recent experiments, a number of current theoretical studies are aimed at reproducing the known cross-section data and further extrapolating the calculations into the region of spherical superheavy nuclei. Publications to that effect have been submitted or are in preparation: Adamian *et al.* (1999), Aritomo *et al.* (1999), Cherepanov (1999a, 1999b), Denisov and Hofmann (1999), Giardina *et al.* (2000), and Smolanczuk (1999a). The measured cross sections for the formation of ^{257}Rf ($\sigma=12.5$ nb) up to ^{277}112 ($\sigma=1.0$ pb) are reproduced within about a factor of 2 by the various models. However, there are significant differences in the cross-section values for the synthesis of spherical SHE's beyond $Z=114$. Table I gives some examples of the calculated cross sections for the $1n$ channel using a ^{208}Pb target and beams of ^{76}Ge, ^{82}Se, and ^{86}Kr. The obtained experimental values are also shown.

The models consider fusion of heavy nuclei as a step-by-step process. The following main phases are considered:

(1) capture of projectile and target nucleus;
(2) proton and neutron transfer, surface vibrations;
(3) separation of projectile and target nucleus (quasi-elastic and deep-inelastic processes);
(4) transmission of the fusion barrier;
(5) formation of an excited compound nucleus;
(6) formation of an evaporation residue after cooling of the compound nucleus by emission of neutrons and γ rays in competition with fission.

The probability for the different processes depends on the relative velocity of the reaction partners, the angular momentum, the free reaction energy (excitation energy), and the individual structure of projectile, target, compound, and residual nucleus. These items are not all weighted equally in the various models, which results in the large deviation of the calculated cross sections in the case of far extrapolations. And important details have probably not even been considered yet. As an example of recent improvements, we present a calculation of the fusion barrier according to a model by Möller, Nix, *et al.* (1997) and Möller (1997).

In Fig. 22, fusion barriers are plotted for the reactions ^{76}Ge+^{208}Pb$\rightarrow^{284}$114* and ^{88}Sr+^{208}Pb$\rightarrow^{296}$120*. The calculation was performed using a model of two intersecting spheres and a macroscopic-microscopic approach for the potential energy. The appearance of an inner barrier for these heavy systems is evident. This inner barrier is due to a positive shell-correction energy, which arises at

TABLE I. Experimental and calculated cross sections for the synthesis of superheavy nuclei. The values given are the calculated cross sections for the $1n$ channel using ^{208}Pb target and beams of ^{76}Ge, ^{82}Se, and ^{86}Kr. The experimental data are from Hofmann (1998, ^{289}116) and Ninov *et al.* (1999, ^{293}118). The calculated values are from (a) Adamian *et al.*, 1999; (b) Cherepanov, 1999a, 1999b; (c) Denisov and Hofmann, 1999; (d) Giardina *et al.*, 2000; and (e) Smolanczuk, 1999a.

Isotope	Expt.	(a)	(b)	(c)	(d)	(e)
^{283}114		0.2 pb	0.12 pb	0.35 pb	1.0 pb	0.56 pb
^{289}116	<9.1 pb	15 fb		2–30 pb		7.1 pb
^{293}118	$(2.2^{+2.6}_{-0.8})$ pb	5.1 fb	0.5 pb			670 pb

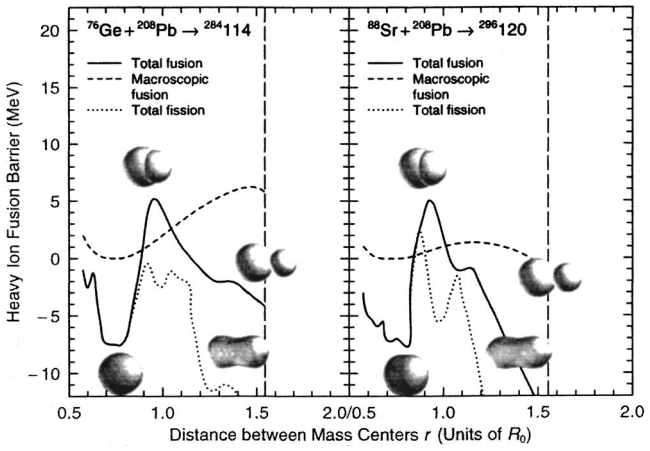

FIG. 22. Calculated barriers for the synthesis of elements 114 and 120 via cold fusion. From Möller *et al.*, 1998.

a configuration reached just before the spherical ground state. It is absent for the lighter elements ($Z<112$) that have a deformed ground-state shape. The inner barrier hinders fusion at energies that are just high enough to reach the contact configuration. The height of the barrier for the fusion of elements 114 to 120 is about 13 MeV above the ground state of the compound nucleus. The existence of the inner barrier may explain the negative result of our search for the 0n channel using the reaction ^{82}Se+^{208}Pb→^{290}116*. On the other hand, the barrier has just the correct height to be in agreement with the successful Berkeley experiment on the synthesis of element 118, which was performed at an excitation energy of 13.3 MeV.

At present, the model is being further developed by taking into account a shape-dependent Wigner term (Möller and Sierk, 1999) in the potential-energy calculation. This is necessary in order to take into account the different N/Z ratios (and thus different number of nucleon pairs) of the reaction partners and the compound nucleus and to provide a smooth behavior of the potential energy at the transition from two separated nuclei to a compound system. As a result, the potential energy increases considerably at the contact point, which leads to the formation of an outer barrier (not shown in Fig. 22) comparable in height to the inner barrier. It is possible that the occurring pocket between the two barriers has a positive influence on the fusion cross section.

Due to the great uncertainty concerning the influence of the various steps in the fusion of heavy elements, more and more precise experimental data are needed. It is especially important that various combinations of projectile and target be investigated, from very asymmetric systems to symmetric ones, and that excitation functions be measured. This provides information on how fast the cross section decreases with increasing energy due to fission of the compound nucleus, and how fast the cross section decreases on the low-energy side due to the fusion barrier. From both slopes, information about the "shape" of the fission and fusion barriers can be obtained. At a high enough cross section, these measurements are complemented by in-beam γ spectroscopy using the recoil-decay tagging method in order to study the influence of angular momentum on the fusion and survival probability.

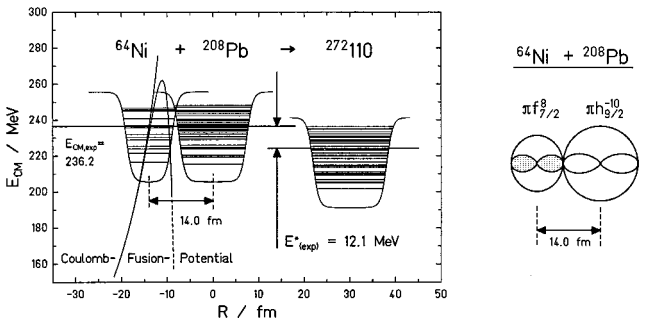

FIG. 23. Energy vs distance diagram for the reaction of an almost spherical ^{64}Ni projectile with a spherical ^{208}Pb target nucleus, resulting in the deformed fusion product ^{271}110 after emission of one neutron. At the center-of-mass energy of 236.2 MeV, the maximum cross section was measured. On the left, the reaction partners are represented by their nuclear potentials (Woods–Saxon) at the contact configuration where the initial kinetic energy is exhausted by the Coulomb potential. On the right, the outermost proton orbitals are shown at the contact point. For the projectile ^{64}Ni, an occupied $1f_{7/2}$ orbit (hatched area) is drawn, and for the target ^{208}Pb an empty $1h_{9/2}$ orbit. The protons circulate in a plane perpendicular to the drawing. The Coulomb repulsion, and thus the probability for separation, is reduced by the transfer of protons. In this model, the fusion is initiated by transfer.

B. Fusion initiated by transfer

In this section, we discuss an additional aspect of the measured excitation functions, which was considered earlier in the literature as a possible mechanism contributing to the fusion of heavy elements (von Oertzen, 1992). In all the investigated cold-fusion reactions up to $Z=112$, the largest cross section was measured "below the barrier." The energy relations that determine the barrier are shown in Fig. 23 for the reaction ^{64}Ni+^{208}Pb, and a barrier based on the model of Bass (1974) is also given. A tunneling process through this relatively high barrier cannot explain the measured cross sections. The conclusion is that additional effects must modify the barrier to make fusion possible. Attempts to improve the heavy-element fusion barrier calculations were discussed in the previous section.

At and below the barrier, the kinetic energy in the center-of-mass system is converted into potential energy, and the reaction partners come to rest in a central collision in a touching configuration. In the case of ^{64}Ni+^{208}Pb, the initial kinetic energy of 236.2 MeV, at which the cross-section maximum was measured, is exhausted by the Coulomb potential at a distance of 14.0 fm between the reaction partners. At that distance, only nucleons on the outer surface are in contact.

We recall that the kinetic energy of orbiting nucleons is low at the surface of the nucleus. Therefore, at the

point of contact of two nuclei in a central collision, the probability of nucleons or pairs of nucleons leaving the orbit of one nucleus and moving into a free orbit of the reaction partner is high. The process is shown schematically on the right side of Fig. 23. An adequate theoretical description could be obtained by use of the two-center shell model (Scharnweber *et al.*, 1971). An approach that reproduces the measured cross sections within the framework of a dinuclear system was presented by Antonenko *et al.* (1995).

Because of the pairing energies and high orbital angular momenta involved, the transfer of pairs is more likely than that of single nucleons. The described process is a frictionless pair transfer occurring at the contact point in a central collision at zero longitudinal momenta in the irradiation of ^{208}Pb targets. This capture process seems already to be disturbed at kinetic energies only slightly higher than those determined by the contact configuration, as discussed by means of the measured excitation functions shown in Fig. 18.

After transfer of two protons from ^{64}Ni to ^{208}Pb, the repulsive Coulomb force is decreased by 4.9%, allowing for the maintenance of the reaction partners in close contact and the continuation of ''fusion initiated by transfer.''

Important factors influencing the cross section at the very beginning of the fusion process are

(1) The probability of a head-on collision.

(2) The probability of proton transfer in competition with the separation of the reaction partners.

The importance of cold multinucleon transfer for the synthesis of heavy elements was realized by von Oertzen (1992). The application of the transfer-initiated fusion model in the description of the low-energy fusion phenomena is based on this work and the experimental result of maximum fusion cross sections at energies well below the Bass barrier. An analysis of transfer data obtained from radiochemical studies was presented by Kratz (1995). Fink *et al.* (1974) considered the possibility of the transfer of complete shells of equal orbital momentum. The transfer of massive clusters for the production of heavy elements, especially neutron-rich species, was considered by Magda and Leyba (1992). The role of nucleon transfer in subbarrier fusion processes was discussed in recent review articles by Balantekin and Takigawa (1998) and by Dasgupta *et al.* (1998).

In the case of reactions with actinide targets and projectiles like ^{48}Ca, the target nucleus is deformed and, at barrier energies, only a fraction of certain orientation will lead to fusion. This orientation effect is absent in the case of spherical ^{208}Pb targets. In addition, the occupation of levels at the Fermi surfaces is such that protons are more likely to transfer from the target to the projectile and thus increase the Coulomb repulsion. This transfer into the ''wrong'' direction was observed using radio chemical methods by Gäggeler *et al.* (1986) and Türler *et al.* (1992). Nevertheless, positive results obtained in Dubna on the synthesis of element 112 and 114 using actinide targets and a ^{48}Ca beam (see Sec. IV.D) seem to establish hot fusion as an alternative path in the synthesis of superheavy elements. Experimentally, the most challenging and exciting task in the near future will be to clarify the advantages of cold and hot fusion reactions for the production of SHE's.

VII. SUMMARY AND OUTLOOK

Experimental work of the last two decades has shown that the cross sections for the synthesis of the heaviest elements decrease almost continuously. However, the recent data on the synthesis of element 114 using hot fusion and 118 using cold fusion seem to break this trend when the region of spherical superheavy elements is reached. A precise theoretical description allowing for an exact enough determination of the optimum choice of the reaction and beam energy is not yet within view. Therefore more experimental data are needed, which cover a wider range of reactions and shift the measurable cross-section limit to lower values. In particular, a confirmation is urgently needed that the region of spherical SHE's has finally been reached and that the exploration of the ''island'' has started. In order to perform such experiments in a reasonable time, a further upgrade of the technical equipment is necessary.

The options for the future are high currents and steady beams running at high duty factors, ideally dc beams. Simultaneously, the use of rare isotopes requires that the consumption of ion-source material be kept at a minimum. The target technique needs to be upgraded in order to withstand the higher beam currents. An effective gas-cooling technique for foil and wheel targets is under development. Liquid targets or gas-jet targets for certain elements may be an alternative. The separator efficiency has to be increased, and a value of more than 50% is feasible. Higher background suppression is mandatory and can be achieved by properly designed dispersive and focusing elements acting as postseparators behind existing devices or by the use of degrader foils in front of the detectors. The detector size needs to be adjusted to the distribution of the reaction products in the focal plane, and the granularity of the detector to the counting rate of reaction products and background. The detector systems used so far could be extended by additional gamma and electron detectors. New devices, like ion traps, could also be installed. For experiments at SHIP, the VEGA project (Gerl *et al.*, 1998), using efficient Ge-gamma detectors, and the construction of the SHIP trap facility (Äystö *et al.*, 1998) are in progress.

These new developments will not only make it possible to perform experiments aimed at synthesizing new elements in reasonable measuring times, but will also allow for a number of other investigations covering reaction physics and spectroscopy.

The experimental program will be significantly influenced by the spectacular results recently obtained at Dubna for the synthesis of elements 112 and 114 and at Berkeley for element 118. In an experiment at SHIP, a first attempt failed to confirm the Berkeley data. However, further experiments are already planned in Berkeley for early in the year 2000. A repetition at SHIP or

even an attempt to synthesize still heavier elements have been postponed until the new data become available, and the SHIP upgrade provides improved sensitivity. The progress towards the exploration of the island of spherical SHE's is difficult to predict. However, despite the exciting new results, many questions of a more general character are still awaiting an answer. The most interesting proposals for upgrades and new experiments around SHIP include in the following:

- Continuation of the SHIP program aimed at synthesizing elements 113 and 114, and possibly 115 and 116, as well, by cold fusion. Data on the synthesis and properties of these elements and nuclei will be important, because they fill the gap between $^{277}112$ and $^{293}118$. Especially in the case of relatively high cross sections for the formation of spherical SHEs, the trend of cross sections and α energies in the transitional region will be needed to understand the reason for that increase.
- Ground state to ground state α decay of even-even nuclei for more accurate evaluation of nuclear binding energies and extraction of shell strength.
- Search for α transitions of even-even nuclei into rotational levels to determine the degree of deformation. These experiments are especially important in the region of deformed nuclei near $N=152$ and 162, where locally high stability is expected due to relatively wide energy gaps between the relevant Nilsson single-particle levels. At a high enough accuracy, the different hexadecapole components may also become measurable. Calculated values are $\beta_4 \approx 0$ near $N=152$ and $\beta_4 \approx -0.09$ near $N=162$ (Möller *et al.*, 1995a, 1995b).
- Fission branching of even-even nuclei for comparison of the extracted partial fission half-lives with the results of calculations. Fission half-lives are the most sensitive parameter for testing the predictions of nuclear models with respect to the stability of SHE's.
- Gamma and conversion-electron spectroscopy of separated fusion products. Many isotopes of heavy nuclei have considerable β or electron-capture branching, are formed and separated in long-lived isomeric states, or have their excited levels populated by α decay. Therefore partial level diagrams could be established even in the case of small production cross sections using highly efficient γ or electron detectors. For these applications, as in the case of experiments using SHIPtrap (see the next item), the detectors are mounted in a region of low background behind SHIP, and the highest currents can be used to produce the wanted species.
- The installation of an ion trap behind SHIP will considerably widen the possibilities for the investigation of separated nuclei. For example, precise mass measurements can be performed and the electronic configuration of heavy ions can be studied by laser spectroscopy. These methods are well applicable to the study of relatively long-lived species, as predicted for isotopes close to the center region of SHE's. More details of planned experiments are given in the SHIPtrap proposal (Äystö *et al.*, 1998).
- The measurement of excitation functions is critical both for estimating the optimum beam energy for the production of new elements and for learning more about the reaction mechanism. In particular, the reactions $^{64}Ni+^{209}Bi \rightarrow ^{272}111+1n$ and $^{70}Zn+^{208}Pb \rightarrow ^{277}112+1n$ need to be studied for optimum preparation of experiments searching for elements 113 and 114 by cold fusion. A variation of the beam energy for the reaction $^{86}Kr+^{208}Pb \rightarrow ^{293}118+1n$ is in preparation at Berkeley.
- In order to better understand the cold-fusion reaction mechanism on a microscopic level, it is also important to investigate reactions using neighboring projectile or target nuclei, thus making small but well-defined changes. For example, the reason for the cross-section increase in the production of element 110 isotopes when ^{64}Ni is used instead of ^{62}Ni is not yet understood. An explanation would help in clarifying the usefulness of more neutron-rich, radioactive projectiles for the synthesis of SHE's.
- The study of fusion barriers and deexcitation of the compound nucleus can be complemented by the investigation of the radiative capture process and the use of less bound neutron-deficient projectiles. The former reaction type is possible at free reaction energies less than the neutron-binding energy, and the latter would lead to an increase in the excitation energy at the fusion barrier.
- A possible alternative to synthesizing SHE's by cold fusion is hot fusion using actinide targets. This type of reaction has not yet been investigated at SHIP, because of low transmission values. Excitation functions especially are poorly known. The investigation of more neutron-rich, longer-lived isotopes using stable projectiles is only possible with actinide targets. It could be advantageous in increasing element numbers to make use of the decreasing excitation energy at the fusion barrier. The use of the strongly bound ^{48}Ca as a projectile is especially promising as was demonstrated by the experiments at Dubna (see Sec. IV.D).
- The reaction studies should be completed by investigating symmetric reactions. In this case, the projectile and target nuclei are close to the magic proton and neutron shell $Z=50$ and $N=82$, resulting in cold compound nuclei. In spite of the great amount of extra push energy predicted for symmetric reactions (Fröbrich, 1988), the use of closed-shell nuclei as projectile and target could result in interesting entrance-channel effects, because in this case the fusion may be considered as an inverse fission process. The proposed reactions range from $^{124}Sn+^{124}Sn \rightarrow ^{248}Fm^*$ to $^{136}Xe+^{136}Xe \rightarrow ^{272}Hs^*$. The latter reaction would be the ideal case for the use of a gas-jet target.
- The development of radioactive beams with energies near the Coulomb barrier is in progress (Geissel *et al.*, 1995; Münzenberg, 1998). With respect to the previous item, the doubly magic nucleus ^{132}Sn is of special interest. Neutron-rich radioactive isotopes of lighter elements will be used in studies of the transition region from deformed nuclei at $N=162$ to spherical nuclei at $N=184$. The reaction mechanism can be investigated across wider isotopic chains. Projects have just started or are under discussion at GANIL, France (SPIRAL); Catania, Italy (EXCYT); JHF, Tokyo, Japan (E-arena);

Oak Ridge and Argonne, United States (RIA); and Munich, Germany (MAFF). These facilities will provide beams of extremely neutron-rich nuclei with intensities of 10^7/s and, for some isotopes, possibly up to 10^{11}/s.

• Study of the deexcitation of the compound nucleus by in-beam γ spectroscopy using the recoil-tagging technique. This method was recently applied at Argonne and at Jyväskylä for studying the 3-μb $2n$ evaporation channel of the reaction $^{48}Ca+^{208}Pb\rightarrow^{256}No^*$. With the use of the new, highly efficient γ-detector arrays and a highly efficient recoil separator, these experiments could be extended to in-beam studies of lawrencium and possibly rutherfordium isotopes.

• Experiments using the inverse reaction (beams of lead or uranium isotopes and targets of light elements) have different kinematic properties. The kinetic energy of the reaction products is high, and their momentum is directed into a more narrow cone. These properties may allow for an identification in flight at almost 100% transmission of the separator. The method has the advantage of being independent from the half-life, which could become especially useful in the case of long half-lives when the correlation method fails.

• Finally, the chemistry of the transactinide elements is of particular interest (Schädel, 1995). By using SHIPtrap, the possible studies will be extended considerably over conventional radiochemical methods. The chemical behavior of relatively short-lived isotopes ($T_{1/2}<100$ ms) can be investigated. The study of the reaction kinematics using trapped ions will also become possible.

One can hope that, during the coming years, more data will promote a better understanding of the stability of the heaviest elements and the processes that lead to fusion. A microscopic description of the fusion process will be needed for an effective explanation of the measured phenomena in the case of low dissipative energies. Then the relationships between fusion probability and stability of the fusion products may also become apparent.

An opportunity for the continuation of experiments in the region of SHE's at decreasing cross sections will be afforded by further accelerator developments. Radioactive beams and high-current beams are the options for the future. At increased beam currents, values of tens of particle μA's may become possible, the cross-section level for the performance of experiments can be shifted down into the region of femtobarns, and excitation functions can be measured on the level of tenths of picobarns. The high currents, in turn, require the development of a new target and improvement of the separator.

The half-lives of SHE's are expected to be relatively long. Based on nuclear models, which are effective predictors of half-lives in the region of the heaviest elements, values from microseconds to years have been calculated for various isotopes. This wide range of half-lives encourages the application of a wide variety of experimental methods in the investigation of SHE's, from the safe identification of short-lived isotopes by recoil-separation techniques to atomic physics experiments on trapped ions, and to the investigation of chemical properties of long-lived isotopes.

VIII. NOTE ADDED IN PROOF

An experiment was performed at the GSI SHIP during May 2000 aiming to confirm the synthesis of $^{277}112$. We used the same reaction as in our previous irradiation, $^{70}Zn+^{208}Pb\rightarrow^{278}112^*$ (see Sec. III.A). However, in the new experiment a beam energy of 346.1 MeV was chosen resulting in an excitation energy of 12.0 MeV, 2.0 MeV higher than in the first experiment.

During an irradiation time of 19 days we collected a total of 3.5×10^{18} projectiles. One decay chain was observed. The measured data and our assignment are given in Fig. 24. The first two α decays have energies of 11.17 and 11.20 MeV, respectively, which are succeeded by an α of only 9.18 MeV, an energy step by about 2 MeV. Correspondingly, the lifetime increases by about five orders of magnitude between the second and third α decay. This decay pattern is in agreement with the one observed for chain 2 in our first experiment (see Figs. 4 and 5). It was explained as the result of a local minimum of the shell correction energy at neutron number $N=162$ which is crossed by the α decay of $^{273}110$.

The α energy of 9.18 MeV for the decay of ^{269}Hs is identical within the detector result with the value of 9.17 MeV obtained in chain 1 of our previous experiment. A

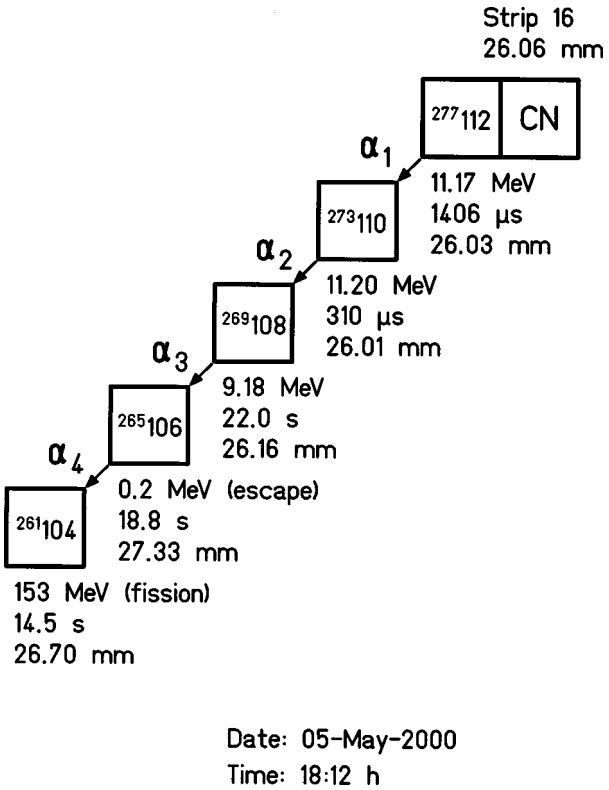

FIG. 24. Decay chain of $^{277}112$ observed in the recent experiment at the GSI SHIP. The data given are energies of the detector signals in MeV, time differences, and positions in vertical direction from the bottom of detector strip number 16.

TABLE II. Names and symbols of the transfermium elements. Column 3: Names finally accepted by the IUPAC General Assembly in August 1997; Columns 4 and 5: Names previously in use.

Z	Period of discovery	IUPAC 1997 (Currently accepted)	IUPAC 1994	Other names suggested or previously in use
101	1955–58	Mendelevium (Md)	Mendelevium (Md)	
102	1958–65	Nobelium (No)	Nobelium (No)	
103	1961–71	Lawrencium (Lr)	Lawrencium (Lr)	
104	1964–69	Rutherfordium (Rf)	Dubnium (Db)	Rutherfordium (Rf), Kurchatovium (Ku)
105	1968–70	Dubnium (Db)	Joliotium (Jl)	Hahnium (Ha), Nielsbohrium (Ns)
106	1974	Seaborgium (Sg)	Rutherfordium (Rf)	
107	1981	Bohrium (Bh)	Bohrium (Bh)	Nielsbohrium (Ns)
108	1984	Hassium (Hs)	Hahnium(Hn)	
109	1982	Meitnerium (Mt)	Meitnerium (Mt)	
110	1994	unnamed		
111	1994	unnamed		
112	1996	unnamed		

new result is the occurrence of fission ending the new chain at ^{261}Rf. Fission was not yet known from ^{261}Rf, but is likely to occur taking into account the high fission probabilities of the neighboring even isotopes (Fig. 3). The three lifetimes of ^{261}Rf measured in our decay chains are all significantly shorter than the literature value of 94 s. The mean value obtained from the three decay chains is (17^{+24}_{-6}) s. Moreover, the α energy of 8.52 MeV measured for ^{261}Rf in chain 2 is 0.24 MeV higher than the literature value of 8.28 MeV. The data suggest that in the decay chain from ^{277}112 a level in ^{261}Rf is dominantly populated different from the one observed in a direct production of ^{261}Rf using the reaction $^{248}\mathrm{Cm}+^{18}\mathrm{O}\rightarrow^{266}\mathrm{Rf}^*$. Because the α energy of 8.52 MeV fits better into the systematics of ground-state α energies, we tentatively assign the two α decays and the one fission event measured in our ^{277}112 decay chains to the ground state of ^{261}Rf. The deduced fission branching is $0.33^{+0.33}_{-0.18}$ and the partial fission half-life is (36^{+62}_{-24}) s.

A cross section of $(0.5^{+1.1}_{-0.4})$ pb was measured for the new data point at 12.0 MeV excitation energy. This value fits well into the systematics of cross sections shown in Fig. 18. A cross section increase with increasing beam energy as predicted by theoretical investigations was not observed. During our experiment we also used for a period of 7 days a beam energy of 343.8 MeV, the same as in our previous irradiation. No new event was measured at a beam dose of 1.2×10^{18}. A new mean value of $(0.7^{+0.9}_{-0.5})$ pb follows for the data point at 10.0 MeV excitation energy. Finally, we irradiated a $^{238}UF_4$ target for a period of 3 days. The resulting compound nucleus would be ^{308}122. The aim of this experiment was to use the available ^{70}Zn beam for testing a possible relatively high cross section for the synthesis of superheavy nuclei close to the double magic nucleus predicted at $Z=120$ and $N=184$. The experiment was performed at a beam energy of 370.3 MeV. This energy was estimated so that a touching configuration could be reached under the assumption of a spherical ^{238}U target nucleus. The resulting excitation energy of the compound nucleus would be 18.6 MeV at the target's center thickness. At a beam dose of 0.6×10^{18} particles, we did not observe a decay chain which could be assigned to a superheavy nucleus. A deduced cross-section limit is 7.2 pb at a 68% confidence level.

The recent experiment at SHIP was performed by S. Hofmann, F.P. Heßberger, D. Ackermann, B. Kindler, J. Kojouharova, B. Lommel, R. Mann, G. Münzenberg, S. Reshitko, H.J. Schött (GSI Darmstadt); A. Popeko, A. Yeremin (JINR Dubna); S. Antalic, P. Cagarda, S. Śaro (University Bratislava); H. Kettunen, M. Leino, J. Uusitalo (University Jyväskylä).

ACKNOWLEDGMENTS

The recent experiments at SHIP were performed in collaboration with D. Ackermann, P. Armbruster, H. G. Burkhard, H. Folger, F. P. Heßberger, B. Kindler, B. Lommel, V. Ninov, S. Reshitko, H. J. Schött, C. Stodel (GSI Darmstadt), A. N. Andreyev, A. Yu. Lavrentev, A. G. Popeko, A. V. Yeremin (FLNR-JINR Dubna), S. Antalic, P. Cagarda, R. Janik, S. Śaro (University of Bratislava), and M. Leino, University of Jyväskylä. The most important prerequisite for the experimental program was a stable and high-current beam of accurate energy from the UNILAC. It is a great pleasure to thank for their contributions the people from the ion-source group, the accelerator, the target laboratory, and the department of experimental electronics and data acquisition. Concerning the theory of the synthesis and stability of SHE's, we are particularly grateful for fruitful discussions with N. V. Antonenko, E. A. Cherepanov, S. Ćwiok, V. Yu. Denisov, W. Greiner, P. Möller, A. K. Nasirov, W. Nazarewicz, W. Nörenberg, W. von Oertzen, Yu. Ts. Oganessian, W. Reisdorf, K. H.

Schmidt, R. Smolanczuk, and A. Sobiczewski. We thank Celine Détraz for careful editing of the English version of the article.

APPENDIX: THE NAMING OF ELEMENTS

Obviously, the extension of the Periodic Table is always an effort requiring the most sensitive experimental equipment available. Exploring the stability limits may sometimes lead to results, that do not stand up to a critical test later on. This was the case when the Periodic Table was established independently by the Russian scientist Dmitri Iwanowich Mendeleev and by the German scientist Lothar Meyer, and the task was to fill the gaps between known elements.

The synthesis and the identification of the transuranium elements impressively reflect the wide variety of experimental methods that have been developed and applied since first attempts were made by Enrico Fermi, Emilio Segrè, and co-workers (1934) in Rome, shortly after the discovery of the neutron.

For the synthesis of heavy nuclei, the cold fusion reaction with lead targets was introduced by Oganessian, Iljinov, *et al.* (1975) and Oganessian, Demin, *et al.* (1975). For awhile, it successfully replaced the method of hot-fusion reaction using actinide targets. Cold fusion required the development of more powerful ion sources and accelerators for the heavier ions needed in the reactions with lead. Chemical separation techniques and mechanical transport systems were replaced by electromagnetic recoil separators, which reduced the separation time to a few microseconds. The resolving power of detectors was increased, and the introduction of position-sensitive detectors allowed for the observation of generic parent-daughter decays to known isotopes over a wide range of half-lives. The electronic data acquisition systems were miniaturized, allowing for the use of multiple parameter detector systems. The resulting large volume of data was analyzed by fast computers.

These numerous ground breaking technical developments resulted in the unequivocal identification of element $Z=109$, based only on the observation of a single atom (Münzenberg *et al.*, 1982). Certainly it was fortunate that the identification method used proved to be ideal for observing the decay of this isotope.

The identification of new elements has not always been so straightforward and convincing. This has unfortunately led to controversy in the past. Claims of the discovery of a new element and therefore the right to name it have attracted considerable attention. For this reason, IUPAC and IUPAP, the International Unions of Pure and Applied Chemistry/Physics, decided to establish the Transfermium Working Group to consider questions of priority in the discovery of elements $Z>100$. A report of their extensive work was published by Barber *et al.* (1992), and names were recommended on the basis of this report for elements 101 to 109 (IUPAC, 1994). Although it attempted to find a compromise, the proposed list was not accepted in all details by the research groups at Berkeley (Ghiorso and Seaborg, 1993), Dubna (Oganessian and Zvara, 1993), and Darmstadt (Armbruster *et al.*, 1993). As a consequence, a new list was created and accepted at the IUPAC General Assembly in August 1997 (IUPAC, 1997). It was made public in a February 1997 press release.

In Table II, we summarize the names and symbols of elements $Z=101$ to 109, which have now found acceptance. We also present the names that had been previously used. Currently the naming of elements 110 to 112 is in progress. No names have been proposed yet for any of the elements beyond 112.

There was a great deal of discontent about the way names were eventually assigned to elements 102 to 109, and IUPAC was determined not to let this occur again with the latest elements. The aim was therefore to make the process of naming an element as open and as free from objection as possible. An IUPAC/IUPAP Joint Working Party composed of independent experts was set up in January 1999 to judge the validity and relative value of claims for priority for elements 110 to 112. Having reviewed the relevant literature pertaining to the different claims, the Joint Working Party is at present (December 1999) preparing a report for publication. All contending institutes will be sent reprints at the time of submission with the understanding that each might choose to submit its own comments for concurrent publication. The procedure allows for the highest possible transparency and makes it possible to reach an agreement in controversial cases before any names are proposed and start to circulate. The institute that is assigned priority for the discovery of an element will finally be approached for suggestions of names.

The criteria that must be satisfied in order for the discovery of a new element to be recognized were established by the 1992 Transfermium Working Group report. These criteria served as a guide for the new Joint Working Party and will probably also be the basis for the work of similar committees in the future. One criterion of a more general nature is the reproducibility of an experimental result, and the Transfermium Working Group suggested that no new element should be officially recognized until the data have been reproduced. However, a need for repetition could be waived in the cases in which the data are of such a nature that no reasonable doubt is possible and a repetition of the experiment would imply an unreasonable burden.

Concerning the recent results on elements 111 and 112 in Darmstadt (in the case of $^{269}110$ and $^{271}110$ redundancy already exists), 114 in Dubna, and 118 in Berkeley, our opinion is that the experiments could be repeated without unreasonably strenuous efforts. The cross sections are in the range of one picobarn, which means a production rate of about one event per week with the experimental setups presently available. The lifetimes are in an easily accessible window between 100 μs and 10 min.

Experiments searching for effects at the limits of detectability always carry a risk of being erroneous, although it is difficult to give a probability value describing to what extent they are erroneous or correct.

Statistical fluctuations alone are not enough to characterize the good or poor quality of a measurment. Early results can be proven or disproven only by additional experiments, preferably with different techniques or with a variation of parameters such as the beam energy.

In this procedure, however, a clear disproof is more difficult to achieve than a proof. Experiments are already planned for the year 2000 aimed at confirming the synthesis of elements 111 and 112 at Darmstadt and of 118 at Berkeley using improved equipment. The experiments at Dubna will be continued using a more intense ^{48}Ca beam and different actinide targets. Investigation of the synthesis of superheavy elements is also planned at the laboratories of GANIL in France, and RIKEN in Japan. These developments are therefore promising, as they will, in the near future, not only confirm whether the recent results were correct, but also provide important new data that will help to better localize and further explore the region of superheavy nuclei.

REFERENCES

Adamian, G. G., N. V. Antonenko, and W. Scheid, 1999, Institüt für Theoretische Physia der Justus-Liebig-Universität Giessen, Germany, preprint.

Ahmad, I., R. R. Chasman, A. M. Friedman, and W. S. Yates, 1990, Phys. Lett. B **251**, 338.

Ahmad, I., A. M. Friedman, R. R. Chasman, and S. W. Yates, 1977, Phys. Rev. Lett. **39**, 12.

Andreyev, A. N., D. D. Bogdanov, V. I. Chepigin, M. Florek, F. P. Heßberger, *et al.*, 1992a, in *Proceedings of the Sixth International Conference on Nuclei Far From Stability* and the *Ninth International Conference on Atomic Masses and Fundamental Constants*, Bernkastel-Kues, Germany, July 19–24, 1992, Institute of Physics Conference Series No. 132, edited by R. Neugart and A. Wöhr (IOP Publishing, Bristol/Philadelphia), p. 423.

Andreyev, A. N., D. D. Bogdanov, V. I. Chepigin, M. Florek, A. P. Kabachenko, O. N. Malyshev, S. Sharo, G. M. Ter-Akopian, M. Veselsky, and A. V. Yeremin, 1992b, in *Proceedings of the Sixth International Conference on Nuclei Far From Stability* and the *Ninth International Conference on Atomic Masses and Fundamental Constants*, Bernkastel-Kues, Germany, July 19–24, 1992, Institute of Physics Conference Series No. 132, edited by R. Neugart and A. Wöhr (IOP Publishing, Bristol/Philadelphia), p. 759.

Andreyev, A. N., D. D. Bogdanov, V. I. Chepigin, A. P. Kabachenko, O. N. Malyshev, R. N. Sagaidak, G. M. Ter-Akopian, M. Veselsky, and A. V. Yeremin, 1993, Z. Phys. A **345**, 247.

Angert, N., L. Dahl, J. Glatz, J. Klabunde, M. Müller, U. Ratzinger, H. Deitinghoff, H. Klein, and A. Schempp, 1989, GSI Report **89-1**, 372.

Aritomo, Y., T. Wada, M. Ohta, and Y. Abe, 1999, Phys. Rev. C **59**, 796.

Antonenko, N. V., E. A. Cherepanov, A. K. Nasirov, V. P. Permjakov, and V. V. Volkov, 1995, Phys. Rev. C **51**, 2635.

Armbruster, P., J. Eidens, J. W. Grueter, H. Lawin, E. Roeckl, and K. Sistemich, 1971, Nucl. Instrum. Methods **91**, 499.

Armbruster, P., F. P. Heßberger, S. Hofmann, M. Leino, G. Münzenberg, W. Reisdorf, and K. H. Schmidt, 1993, Prog. Part. Nucl. Phys. **31**, 241.

Audi, G., and A. H. Wapstra, 1993, Nucl. Phys. A **565**, 1.

Äystö, J., H. Backe, G. Bollen, F. Bosch, J. Dilling, A. Dretzke, T. Faestermann, J. Friese, *et al.*, Proposal for SHIPtrap, a capture and storage facility at GSI for heavy radionuclides from SHIP, Gesellschaft für Schwerionenforschung, April 1998, 1, unpublished; see www.gsi.de/~shiptrap.

Balagna, J. P., G. P. Ford, D. C. Hoffman, and J. D. Knight, 1971, Phys. Rev. Lett. **26**, 145.

Balantekin, A. B., and N. Takigawa, 1998, Rev. Mod. Phys. **70**, 77.

Barber, R. C., N. N. Greenwood, A. Z. Hrynkiewicz, Y. P. Jeannin, M. Lefort, M. Sakai, I. Ulehla, A. H. Wapstra, and D. H. Wilkinson, 1992, Prog. Part. Nucl. Phys. **29**, 453.

Bass, R., 1974, Nucl. Phys. A **231**, 45.

Berdichevsky, D., A. Lukasiak, W. Nörenberg, and P. Rozmej, 1989, Nucl. Phys. A **502**, 395c.

Berthes, G., 1987, Ph.D. thesis (Gesellschaft für Schwerionenforschung) GSI Report **87-12**.

Bohr, A., and B. R. Mottelson, 1969, *Nuclear Structure I, Single-Particle Motion* (Benjamin, New York/Amsterdam).

Bossler, J., H. Emig, M. Khaouli, K. Leible, C. D. Mühle, S. Schennach, H. Schulte, P. Spädtke, and K. Tinschert, 1997, GSI Report **97-1**, 155.

Chasman, R. R., and I. Ahmad, 1997, Phys. Lett. B **392**, 255.

Chasman, R. R., I. Ahmad, A. M. Friedman, and J. R. Erskine, 1977, Rev. Mod. Phys. **49**, 833.

Cherepanov, E. A., 1999a, Pramana J. Phys **53**, 619.

Cherepanov, E. A., 1999b, private communication.

Ćwiok, S., J. Dobaczewski, P. H. Heenen, P. Magierski, and W. Nazarewicz, 1996, Nucl. Phys. A **611**, 211.

Ćwiok, S., S. Hofmann, and W. Nazarewicz, 1993, Joint Institute for Heavy Ion Research, Oak Ridge, TN 37831, USA, Doc. no. 93-18, p. 1.

Ćwiok, S., S. Hofmann, and W. Nazarewicz, 1994, Nucl. Phys. A **573**, 356.

Ćwiok, S., and W. Nazarewicz, 1999, private communication.

Ćwiok, S., V. V. Pashkevich, J. Dudek, and W. Nazarewicz, 1983, Nucl. Phys. A **410**, 254.

Ćwiok, S., P. Rozmej, A. Sobiczewski, and Z. Patyk, 1989, Nucl. Phys. A **491**, 281.

Dasgupta, M., D. J. Hinde, N. Rowley, and A. M. Stefanini, 1998, Annu. Rev. Nucl. Part. Sci. **48**, 401.

Davids, C. N., 1992, Nucl. Instrum. Methods Phys. Res. B **70**, 358.

Denisov, V. Yu., and S. Hofmann, 1999, Phys. Rev. C **61**, 034606.

Fermi, E., E. Amaldi, O. D'Agostino, F. Rasetti, and E. Segrè, 1934, Proc. R. Soc. London, Ser. A **146**, 483.

Fink, H. J., W. Greiner, R. K. Gupta, S. Liran, H. J. Maruhn, W. Scheid, and O. Zohni, 1974, in *Proceedings of the International Conference on Reactions between Complex Nuclei*, Nashville, Tennessee, June 10–14, 1974, edited by R. L. Robinson, F. K. McGowan, J. B. Ball, and J. H. Hamilton (North-Holland, Amsterdam/American Elsevier, New York), p. 21.

Fiset, E. O., and J. R. Nix, 1972, Nucl. Phys. A **193**, 647.

Flerov, G. N., and G. M. Ter-Akopian, 1983, Rep. Prog. Phys. **46**, 817.

Folger, H., W. Hartmann, F. P. Heßberger, S. Hofmann, J. Klemm, G. Münzenberg, V. Ninov, W. Thalheimer, and P. Armbruster, 1995, Nucl. Instrum. Methods Phys. Res. A **362**, 64.

Fröbrich, P., 1988, Phys. Lett. B **215**, 36.

Gäggeler, H., 1999, Oral presentation at *Third International Conference on Modern Problems of Nuclear Physics*, Bukhara, Uzbekistan, August 23–27, 1999, unpublished.
Gäggeler, H., W. Brüchle, M. Brügger, M. Schädel, K. Sümmerer, G. Wirth, J. V. Kratz, M. Lerch, Th. Blaich, G. Herrmann, *et al.*, 1986, Phys. Rev. C **33**, 1983.
Gamov, G., 1930, Proc. R. Soc. London, Ser. A **126**, 632.
Geissel, H., G. Münzenberg, and K. Riisager, 1995, Annu. Rev. Nucl. Part. Sci. **45**, 163,
Geller, R., P. Ludwig, and G. Melin, 1992, Rev. Sci. Instrum. **63**, 2795.
Gerl, J., H. Grawe, E. Roeckl, and H. J. Wollersheim for the VEGA Collaboration, *VEGA, a Proposal for Versatile and Efficient GAmma-detectors*. Gesellschaft für Schwerionenforschung, October 1998, 1, unpublished.
Ghiorso, A., 1970, in *Proceedings of the Robert A. Welch Foundation Conference on Chemical Research XIII, The Transuranium Elements—The Mendeleev Centennial*, Houston, Texas, November 17–19, 1969 (Robert A. Welch Foundation, Houston, Texas), p. 143.
Ghiorso, A., M. Nurmia, J. Harris, K. Eskola, and P. Eskola, 1969, Phys. Rev. Lett. **22**, 1317.
Ghiorso, A., and G. T. Seaborg, 1993, Prog. Part. Nucl. Phys. **31**, 233.
Ghiorso, A., S. Yashita, M. E. Leino, L. Frank, J. Kalnins, P. Armbruster, J-P. Dufour, and P. K. Lemmertz, 1988, Nucl. Instrum. Methods Phys. Res. A **269**, 192.
Ghiorso, A., *et al.*, 1995a, Nucl. Phys. A **583**, 861c.
Ghiorso, A., *et al.*, 1995b, Phys. Rev. C **51**, R2293.
Giardina, G., S. Hofmann, A. I. Muminov, and A. K. Nasirov, 2000, Eur. Phys. J. (in press).
Göppert-Mayer, M., 1948, Phys. Rev. **74**, 235.
Göppert-Mayer, M., and J. H. D. Jensen, 1955, *Elementary Theory of Nuclear Shell Structure* (Wiley, New York).
Gregorich, K., 1999, Oral presentation, *First International Conference On the Chemistry and Physics of the Transactinide Elements*, Seeheim, Germany, September 26–30, 1999, unpublished.
Gregorich, K. E., A. Ghiorso, I. Y. Lee, D. M. Moltz, E. B. Norman, Z. Q. Xie, J. G. Kalnins, and C. E. Taylor, 1996, "The Berkeley Gas-Filled Separator (BGS), A New Separator for Compound Nucleus Recoils," Lawrence Berkeley National Laboratory, Berkeley, California, unpublished.
Hahn, O., and F. Strassmann, 1939, Naturwissenschaften **27**, 11.
Haxel, F. P., J. H. D. Jensen, and H. D. Suess, 1949, Phys. Rev. **75**, 1769.
Heßberger, F. P., S. Hofmann, V. Ninov, P. Armbruster, H. Folger, G. Münzenberg, H. J. Schött, A. G. Popeko, A. V. Yeremin, A. N. Andreyev, and S. Śaro, 1997, Z. Phys. A **359**, 415.
Hoffman, D. C., 1974, J. Alloys Compd. **213/214**, 67.
Hofmann, S., 1994, J. Alloys Compd. **213/214**, 74.
Hofmann, S., 1998, Rep. Prog. Phys. **61**, 639.
Hofmann, S., W. Faust, G. Münzenberg, W. Reisdorf, P. Armbruster, K. Güttner, and H. Ewald, 1979, Z. Phys. A **291**, 53.
Hofmann, S., F. P. Heßberger, V. Ninov, P. Armbruster, G. Münzenberg, C. Stodel, A. G. Popeko, A. V. Yeremin, S. Śaro, and M. Leino, 1997, Z. Phys. A **358**, 377.
Hofmann, S., G. Münzenberg, F. P. Heßberger, and H. J. Schött, 1984, Nucl. Instrum. Methods Phys. Res. A **223**, 312.
Hofmann, S., *et al.*, 1995a, Z. Phys. A **350**, 277.
Hofmann, S., *et al.*, 1995b, Z. Phys. A **350**, 281.
Hofmann, S., *et al.*, 1996, Z. Phys. A **354**, 229.
Hulet, E. K., J. F. Wild, R. J. Dougan, R. W. Lougheed, J. H. Landrum, A. D. Dougan, M. Schädel, R. L. Hahn, and P. A. Baisden, 1986, Phys. Rev. Lett. **56**, 313.
IUPAC, Commission on Nomenclature of Inorganic Chemistry, 1994, Pure Appl. Chem. **66**, 2419.
IUPAC, Commission on Nomenclature of Inorganic Chemistry, 1997, Chem. Eng. News **75**, 12.
Keller, J. V., H. G. Clerc, K. H. Schmidt, Y. K. Agarwal, F. P. Heßberger, R. Hingmann, G. Münzenberg, W. Reisdorf, and C. C. Sahm, 1983, Z. Phys. A **311**, 243.
Kratz, A. T., 1995, Radiochim. Acta **70/71**, 147–161.
Kruppa, A. T., M. Bender, W. Nazarewicz, P. G. Reinhard, T. Vertse, and S. Ćwiok, 2000, Phys. Rev. C **61**, 034313.
Kutner, V. B., *et al.*, 1998, in *Proceedings of the 15th International Conference on Cyclotrons and Their Applications*, Caen, France, June 14–19, 1998, edited by E. Baron and M. Lieuvin (IOP, Bristol), p. 405.
Lalazissis, G. A., M. M. Sharma, P. Ring, and Y. K. Gambhir, 1996, Nucl. Phys. A **608**, 202.
Lazarev, Yu. A., *et al.*, 1993, in *Proceedings of the International School Seminar on Heavy Ion Physics*, Dubna, Russia, May 10–15, 1993, edited by Yu. Ts. Oganessian, Yu. E. Penionzhkevich, and R. Kalpakchieva (Joint Institute for Nuclear Research, Dubna), Vol. II, p. 497.
Lazarev, Yu. A., *et al.*, 1994, Phys. Rev. Lett. **73**, 624.
Lazarev, Yu. A., *et al.*, 1995, Phys. Rev. Lett. **75**, 1903.
Lazarev, Yu. A., *et al.*, 1996, Phys. Rev. C **54**, 620.
Leino, M., *et al.*, 1999, Acta Phys. Pol. B **30**, 635.
Leino, M., J. Uusitalo, T. Enqvist, K. Eskola, A. Jokinen, K. Loberg, W. H. Trzaska, and J. Äystö, 1994, Z. Phys. A **348**, 151.
Liran, S., and N. Zeldes, 1976, At. Data Nucl. Data Tables **17**, 431.
Magda, M. T., and J. D. Leyba, 1992, Int. J. Mod. Phys. E **1**, 221.
Mairle, G., 1995, Z. Phys. A **350**, 285.
Maruhn, J., and W. Greiner, 1974, Phys. Rev. Lett. **10**, 548.
Meitner, L., and O. R. Frisch, 1939, Nature (London) **143**, 239.
Meldner, H., 1967, in *Proceedings of the International Symposium on Nuclides far off the Stability Line*, Lysekil, Sweden, August 21–27, 1966, edited by W. Forsling, C. J. Herrlander, and H. Ryde, Ark. Fys. **36**, 593.
Miyatake, H., T. Nomura, H. Kawakami, J. Tanaka, M. Oyaizu, K. Morita, T. Shinozuka, H. Kudo, K. Sueki, and Y. Iwata, 1987, Nucl. Instrum. Methods Phys. Res. B **26**, 309.
Möller, P., 1997, private communication.
Möller, P., P. Armbruster, S. Hofmann, and G. Münzenberg, 1998, in *Proceedings of the 2nd International Conference on Exotic Nuclei and Atomic Masses, ENAM-98*, Bellaire, Michigan, June, 1998, AIP Conf. Proc. No. 455, edited by B. M. Sherill, D. J. Morrissey, and C. N. Davids (AIP, Woodbury, NY), p. 698.
Möller, P., and J. R. Nix, 1992, Nucl. Phys. A **549**, 84.
Möller, P., and J. R. Nix, 1994, J. Phys. G **20**, 1681.
Möller, P., J. R. Nix, P. Armbruster, S. Hofmann, and G. Münzenberg, 1997, Z. Phys. A **359**, 251.
Möller, P., J. R. Nix, and K. L. Kratz, 1997, At. Data Nucl. Data Tables **66**, 131.
Möller, P., J. R. Nix, W. D. Myers, and W. J. Świątecki, 1995a, At. Data Nucl. Data Tables **59**, 185.
Möller, P., J. R. Nix, W. D. Myers, and W. J. Świątecki, 1995b, private communication.

Möller, P., J. R. Nix, and W. J. Świątecki, 1989, Nucl. Phys. A **492**, 349.
Möller, P., and A. J. Sierk, 1999, private communication.
Mosel, U., and W. Greiner, 1969, Z. Phys. **222**, 261.
Muntian, I., Z. Patyk, and A. Sobiczewski, 1999, Phys. Rev. C **60**, 041302.
Münzenberg, G., 1988, Rep. Prog. Phys. **51**, 57.
Münzenberg, G., 1997, in *Experimental Techniques in Nuclear Physics*, edited by D. N. Poenaru and W. Greiner (Walter de Gruyter, Berlin/New York), p. 375.
Münzenberg, G., 1998, Philos. Trans. R. Soc. London, Ser. A **356**, 2083.
Münzenberg, G., P. Armbruster, *et al.*, 1982, Z. Phys. A **309**, 89.
Münzenberg, G., P. Armbruster, *et al.*, 1984, Z. Phys. A **317**, 235.
Münzenberg, G., P. Armbruster, *et al.*, 1986, Z. Phys. A **324**, 489.
Münzenberg, G., P. Armbruster, *et al.*, 1987, Z. Phys. A **328**, 49.
Münzenberg, G., P. Armbruster, *et al.*, 1989, Z. Phys. A **333**, 163.
Münzenberg, G., W. Faust, S. Hofmann, P. Armbruster, K. Güttner, and H. Ewald, 1979, Nucl. Instrum. Methods **161**, 65.
Münzenberg, G., F. P. Heßberger, *et al.*, 1986, GSI Annual Report 1985, **GSI-86-1**, 29.
Münzenberg, G., S. Hofmann, F. P. Heßberger, W. Reisdorf, K. H. Schmidt, J. H. R. Schneider, P. Armbruster, C. C. Sahm, and B. Thuma, 1981, Z. Phys. A **300**, 107.
Münzenberg, G., S. Hofmann, *et al.*, 1988, Z. Phys. A **330**, 435.
Münzenberg, G., W. Reisdorf, *et al.*, 1984, Z. Phys. A **315**, 145.
Myers, W. D., and W. J. Świątecki, 1966, Nucl. Phys. **81**, 1.
Myers, W. D., and W. J. Świątecki, 1996, Nucl. Phys. A **601**, 141.
Myers, W. D., and W. J. Świątecki, 1998, Phys. Rev. C **58**, 3368.
Nikolaev, V. S., and I. S. Dmitriev, 1968, Phys. Lett. **28A**, 277.
Nilsson, S. G., 1978, in *Proceedings of the International Symposium on Superheavy Elements*, Lubbock, Texas, edited by M. A. K. Lodhi (Pergamon, New York), p. 237.
Nilsson, S. G., J. R. Nix, A. Sobiczewski, Z. Szymanski, S. Wycech, C. Gustafson, and P. Möller, 1968, Nucl. Phys. A **115**, 545.
Nilsson, S. G., C. F. Tsang, A. Sobiczewski, Z. Szymanski, S. Wycech, C. Gustafson, I. L. Lamm, P. Möller, and B. Nilsson, 1969, Nucl. Phys. A **131**, 1.
Ninov, V., K. E. Gregorich, and C. A. MacGrath, 1998, in *Proceedings of the 2nd International Conference on Exotic Nuclei and Atomic Masses, ENAM-98*, AIP Conference Proceedings No. 455, Bellaire, Michigan, June 23–27, 1988, edited by B. M. Sherril, D. J. Morrissey, and C. N. Davids, (AIP, Woodbury, NY), p. 704.
Ninov, V., F. P. Heßberger, S. Hofmann, H. Folger, G. Münzenberg, P. Armbruster, A. V. Yeremin, A. G. Popeko, M. Leino, and S. Śaro, 1996, Z. Phys. A **356**, 11.
Ninov, V., F. P. Heßberger, S. Hofmann, H. Folger, A. V. Yeremin, A. G. Popeko, A. N. Andreyev, and S. Saro, 1995, Z. Phys. A **351**, 125.
Ninov, V., *et al.*, 1999, Phys. Rev. Lett. **83**, 1104.
Nörenberg, W., 1983, Nucl. Phys. A **409**, 191c.
Oganessian, Yu. Ts., 1995, Nucl. Phys. A **583**, 823.
Oganessian, Yu. Ts., H. Bruchertseifer, *et al.*, 1978, Nucl. Phys. A **294**, 213.
Oganessian, Yu. Ts., A. G. Demin, *et al.*, 1975, Nucl. Phys. A **239**, 157.
Oganessian, Yu. Ts., M. Hussonnois, *et al.*, 1984, Radiochim. Acta **37**, 113.
Oganessian, Yu. Ts., A. S. Iljinov, A. G. Demin, and S. P. Tretyakova, 1975, Nucl. Phys. A **239**, 353.
Oganessian, Yu. Ts., Yu. P. Tretyakov, *et al.*, 1974, JETP Lett. **20**, 265.
Oganessian, Yu. Ts. *et al.*, 1999a, Phys. Rev. Lett. **83**, 3154.
Oganessian, Yu. Ts. *et al.*, 1999b, Joint Institute for Nuclear Research, Dubna, Russia, preprint E7-99-347.
Oganessian, Yu. Ts., A. V. Yeremin, and V. K. Utyonkov, 1998, *International Nuclear Physics Conference INPC/98*, Paris, 1998, Abstracts of contributed papers, edited by N. Labbal and V. Méot, SPN Bruyères-le-Châtel, France. p. 660.
Oganessian, Yu. Ts., A. V. Yeremin, G. G. Gulbekian, *et al.*, 1999, Eur. Phys. J. A **5**, 63.
Oganessian, Yu. Ts., A. V. Yeremin, A. G. Popeko, *et al.*, 1999, Nature (London) **400**, 242.
Oganessian, Yu. Ts., and I. Zvara, 1993, Prog. Part. Nucl. Phys. **31**, 239.
Patyk, Z., and A. Sobiczewski, 1991, Nucl. Phys. A **533**, 132.
Patyk, Z., A. Sobiczewski, P. Armbruster, and K. H. Schmidt, 1989, Nucl. Phys. A **491**, 267.
Paul, M., B. G. Glagola, W. Henning, J. G. Keller, W. Kutschera, Z. Liu, K. E. Rehm, B. Schenk, and R. H. Siemssen, 1989, Nucl. Instrum. Methods Phys. Res. A **277**, 418.
Pfenning, G., H. Klewe-Nebenius, and W. Seelmann-Eggebert, 1998, *Chart of the Nuclides* (Forschungszentrum Karlsruhe, Karlsruhe).
Randrup, J., S. E. Larsson, P. Möller, S. G. Nilsson, K. Pomorski, and A. Sobiczewski, 1976, Phys. Rev. C **13**, 229.
Reiter, P., T. L. Khoo, C. J. Lister, D. Seweryniak, I. Ahmad, M. Alcorta, M. P. Carpenter, J. A. Cizewski, C. N. Davids, and G. Gervais, 1999, Phys. Rev. Lett. **82**, 509.
Rutz, K., M. Bender, T. Bürvenich, T. Schilling, P. G. Reinhard, J. A. Maruhn, and W. Greiner, 1997, Phys. Rev. C **56**, 238.
Săndulescu, A., R. K. Gupta, W. Scheid, and W. Greiner, 1976, Phys. Lett. **60B**, 225.
Śaro, S., *et al.*, 1996, Nucl. Instrum. Methods Phys. Res. A **381**, 520.
Schädel, M., 1995, Radiochim. Acta **70/71** 207.
Schädel, M., W. Brüchle, R. Dressler, *et al.*, 1997, Nature (London) **388**, 55.
Schädel, M., W. Brüchle, B. Schausten, *et al.*, 1997, Radiochim. Acta **77**, 149.
Scharnweber, D., W. Greiner, and U. Mosel, 1971, Z. Phys. **228**, 257.
Schmidt, K. H., C. C. Sahm, K. Pielenz, and H. G. Clerc, 1984, Z. Phys. A **316**, 19.
Seaborg, G. T., and W. D. Loveland, 1990, *The Elements Beyond Uranium* (Wiley, New York).
Smolanczuk, R., 1997, Phys. Rev. C **56**, 812–824.
Smolanczuk, R., 1998, private communication.
Smolanczuk, R., 1999a, Phys. Rev. C **59**, 2634.
Smolanczuk, R., 1999b, Soltan Institute for Nuclear Studies, Warsaw, Poland, preprint SÍNS/Th/2.
Smolanczuk, R., J. Skalski, and A. Sobiczewski, 1995, Phys. Rev. C **52**, 1871.
Smolanczuk, R., and A. Sobiczewski, 1995a, in *Proceedings of the XV. Nuclear Physics Divisional Conference on Low En-*

ergy Nuclear Dynamics, St. Petersburg, Russia, April 18–22, 1995, edited by Yu. Oganessian, R. Kalpakchieva, and W. von Oertzen (World Scientific, Singapore), p. 313.
Smolanczuk, R., and A. Sobiczewski, 1995b, private communication.
Sobiczewski, A., 1994, Phys. Part. Nuclei **25**, 295.
Sobiczewski, A., F. A. Gareev, and B. N. Kalinkin, 1966, Phys. Lett. **22**, 500.
Strutinsky, V. M., 1967, Nucl. Phys. A **95**, 420.
Türler, A., R. Dressler, B. Eichler, H. W. Gäggeler, D. T. Jost, M. Schädel, W. Brüchle, K. E. Gregorich, N. Trautmann, and S. Taut, 1998, Phys. Rev. C **57**, 1648.
Türler, A., *et al.*, 1988, Z. Phys. A **331**, 363.
Türler, A., *et al.*, 1992, Phys. Rev. C **46**, 1364.
von Oertzen, W., 1992, Z. Phys. A **342**, 177.
Wilkins, B. D., E. P. Steinberg, and R. R. Chasman, 1976, Phys. Rev. C **14**, 1832.
Yeremin, A. V., A. N. Andreyev, *et al.*, 1994, Nucl. Instrum. Methods Phys. Res. A **350**, 608.
Yeremin, A. V., D. D. Bogdanov, V. I. Chepigin, V. A. Gorshkov, A. P. Kabachenko, O. N. Malyshev, A. G. Popeko, R. N. Sagaidak, A. Yu. Ter-Akopian, and A. Yu. Lavrentjev, 1997, Nucl. Instrum. Methods Phys. Res. B **126**, 329.
Yeremin, A. V., A. N. Andreyev, *et al.*, 1989, Nucl. Instrum. Methods Phys. Res. A **274**, 528.
Zamfir, N. V., G. Hering, R. F. Casten, and P. Paul, 1995, Phys. Lett. B **357**, 515.